Journal of Medicinal Chemistry

Article

pubs.acs.org/jmc

New Tricks for an Old Natural Product: Discovery of Highly Potent Evodiamine Derivatives as Novel Antitumor Agents by Systemic Structure–Activity Relationship Analysis and Biological Evaluations

Guoqiang Dong,† Shengzheng Wang,† Zhenyuan Miao, Jianzhong Yao, Yongqiang Zhang, Zizhao Guo, Wannian Zhang,* and Chunquan Sheng*

Department of Medicinal Chemistry, School of Pharmacy, Second Military Medical University, 325 Guohe Road, Shanghai 200433, People's Republic of China

Supporting Information

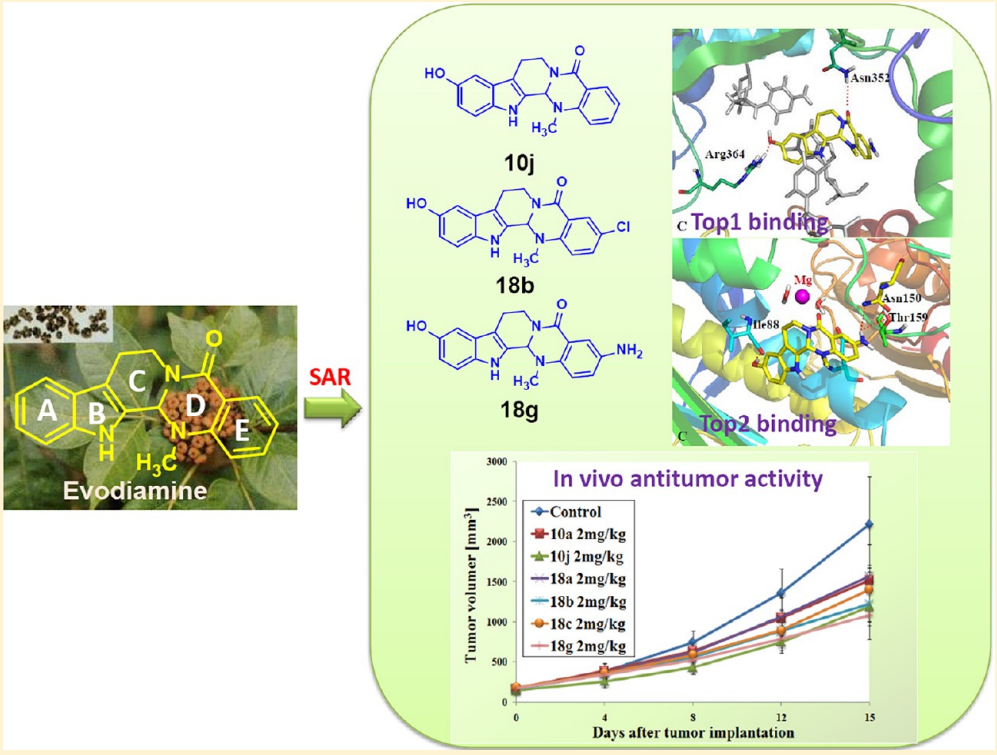

ABSTRACT: Evodiamine is a quinazolinocarboline alkaloid isolated from the fruits of traditional Chinese herb *Evodiae fructus*. Previously, we identified N13-substituted evodiamine derivatives as potent topoisomerase I inhibitors by structure-based virtual screening and lead optimization. Herein, a library of novel evodiamine derivatives bearing various substitutions or modified scaffold were synthesized. Among them, a number of evodiamine derivatives showed substantial increase of the antitumor activity, with GI_{50} values lower than 3 nM. Moreover, these highly potent compounds can effectively induce the apoptosis of A549 cells. Interestingly, further computational target prediction calculations in combination with biological assays confirmed that the evodiamine derivatives acted by dual inhibition of topoisomerases I and II. Moreover, several hydroxyl derivatives, such as 10-hydroxyl evodiamine (**10j**) and 3-amino-10-hydroxyl evodiamine (**18g**), also showed good in vivo antitumor efficacy and low toxicity at the dose of 1 mg/kg or 2 mg/kg. They represent promising candidates for the development of novel antitumor agents.

INTRODUCTION

Natural products have long been an important source of drugs or leads.[1] In the case of antitumor agents, natural products or their synthetic derivatives still comprise more than 50% of the drugs that are used for cancer chemotherapy.[2] Natural products often serve as biologically prevalidated drugs or leads that can lead to discovery of new therapeutic agents and also define novel drug targets.[3] One of the most significant examples is the discovery and development of camptothecin (CPT, **1**)-based antitumor

Received: May 2, 2012
Published: August 6, 2012

dx.doi.org/10.1021/jm300605m | J. Med. Chem. 2012, 55, 7593–7613

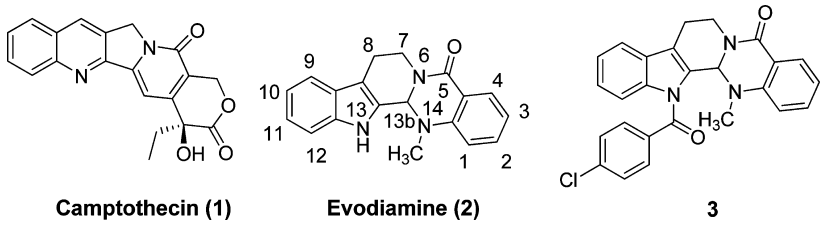

Figure 1. Chemical structures of camptothecin and evodiamine derivatives.

agents.[4] Compound **1** is isolated from the Chinese tree *Camptotheca acuminata* in 1966.[5] Nearly 10 years later, its unique mode of action was found to be selective inhibition of DNA topoisomerase I (Top1).[6] Structural modifications of natural product **1** have generated two effective antitumor agents, namely topotecan (TPT)[7] and irinotecan (IRT),[8] and a number of new drug candidates (e.g., rubitecan,[9] lurtotecan,[10] and exatecan[11]). This successful story highlights the importance of medicinal chemistry and pharmacological efforts on leads from natural products.

Evodiae fructus (Chinese name: Wu-Chu-Yu) is a traditional Chinese herb that has been widely used for gastrointestinal disorders, amenorrhea, headache, and postpartum hemorrhage for thousands of years.[12,13] Evodiamine (**2**, Figure 1), a quinazolinocarboline alkaloid, is the major bioactive constituent isolated from the fruits of *Evodiae fructus*. Compound **2** has shown a wide range of biological activities including anti-inflammatory,[14−16] antiobesity,[17−20] and antitumor[21] effects. In particular, the cytotoxicity of compound **2** on various human cancer cell lines has been extensively studied. Compound **2** has been reported to inhibit the proliferation of a wide variety of tumor cells by inducing their apoptosis.[22−25] It has been recently reported that various molecular mechanism involved in compound **2**-induced apoptosis including caspase-dependent[26−28] and -independent[29] pathways, sphingomyelin pathway,[30] PI3K/Akt/caspase, and Fas-L/NF-κB signaling pathways.[31]

Although the antiproliferative and apoptotic effects of evodimaine have been well studied, it is unsuitable to subject compound **2** for direct clinical development because it exhibits antitumor activity only at micromolar concentrations.[21] The antitumor potency and physicochemical properties of compound **2** remain to be significantly improved. Interestingly, compound **2** has several attractive features as an antitumor lead. First, it shows broad-spectrum antitumor activities. Besides its antiproliferative and apoptotic effects, compound **2** suppresses the invasion and migration of human colon carcinoma cells and melanoma cells to the lung.[32,33] Second, the toxicity of compound **2** is relatively low. It was reported that compound **2** had no toxic effects against normal peripheral blood mononuclear cells,[22] and its LD_{50} value in mice was 77.79 mg/kg.[34] Third, compound **2** is a drug-like molecule that meets the criteria of Lipinski's "rule of five"[35] and also meets the rules for lead-like or fragment-like molecules.[36] The relatively low molecular weight of compound **2** (MW = 303) makes it suitable for further optimization into drug-like candidates because the MW value is often increased during the process of lead-to-candidate.[37,38] In addition, compound **2** has good synthetic accessibility that provides a good opportunity to efficiently generating the library of derivatives.

Despite the promising properties of compound **2** as a good starting point for the development of novel antitumor agents, its medicinal chemistry and molecular targets are poorly understood. Most of the synthetic and medicinal chemistry efforts were focused on rutaecarpine, a N14 analogue of compound **2**.[39−44] In our previous investigations, compound **2** was identified as a novel Top1 inhibitor by structure-based virtual screening.[45] It shares a unique "L type" conformation in the active site of Top1. Only the indole ring of compound **2** intercalates at the DNA cleavage site and forms a hydrogen bond with Arg364. On the basis of the binding mode, preliminary optimization of compound **2** was performed by design and synthesis of a series of *N*-substituted analogues. Compared to compound **2**, the 4-chloro benzoyl derivative **3**, the most active one, showed significantly improved Top1 inhibitory activity, antitumor spectrum, and cytotoxicity.[45]

Inspired by these encouraging results, the present investigation will provide systemic structure−activity relationship (SAR) studies of compound **2**. As a result, a series of highly active derivatives were successfully identified. They showed excellent antiproliferative activities at nanomolar concentrations with a broad spectrum. Particularly, their good in vivo antitumor potency were confirmed in two xenograft models. Moreover, in silico target identification in combination with biological assays indicated that these derivatives acted by dual inhibition of Top1 and Top2.

CHEMISTRY

The synthesis of the target compounds were based on the coupling of ring ABC (substituted 3,4-dihydro-β-carboline) with ring DE (substituted *N*-methyl isatoic anhydride). Ring ABC (**6** and **12**) were prepared by reacting substituted tryptamine **4** with ethyl formate and followed by intramolecular ring closure in the presence of $POCl_3$. Starting from substituted 2-aminobenzoic acid, it was reacted with triphosgene to give isatoic anhydride, which was methylated by CH_3I to afford ring DE (**9** and **13**). Then, intermediate **6** (or **12**) was treated with compound **13** (or **9**) in CH_2Cl_2 at room temperature to give A-ring derivatives **10a−g** (Scheme 1), E-ring derivatives **14a−o** (Scheme 2), and A, E-ring derivatives **17a−e** (Scheme 3) with moderate to high yields. Hydroxyl substituted derivatives, such as **10j**, **11e**, **14p**, **14q**, and **18a−e**, were obtained by demethylation of the corresponding methoxyl derivatives in the presence of BBr_3 and CH_2Cl_2 at low temperature. Subsequently, the hydroxyl group could be alkylated by treating with various haloalkanes and K_2CO_3 to afford compounds **10k−p**. Nitro-substituted derivatives **10h** and **10i** were synthesized by direct nitration of compound **2**. Reduction of the nitro group of compounds **14j** and **17d** using 10% Pd/C and H_2 afforded the amino derivatives **14r** and **18f**. Compound **14r** was further alkylated or acylated to give compounds **15a−d** (Scheme 2).

In the presence of NaH and DMF, several derivatives, such as **10**, **14f**, **14i**, **19**, **21**, and **28**, were treated with 4-chlorobenzoyl chloride to afford the N13-substituted compounds **11a−d**, **11e**, **16a−b**, **20**, **22**, and **29**. Treatment of compound **2** or compound **10g** with Lawesson's reagent afforded the thiocarboyl derivatives **19** and **23**. Reduction of D-ring amide group by $LiAlH_4$ yielded compound **21** (Scheme 4). In the presence of 2-iodoxybenzoic acid (IBX) and DMSO, rutaecarpine analogues **26a−b** were

dx.doi.org/10.1021/jm300605m | J. Med. Chem. 2012, 55, 7593−7613

Scheme 1[a]

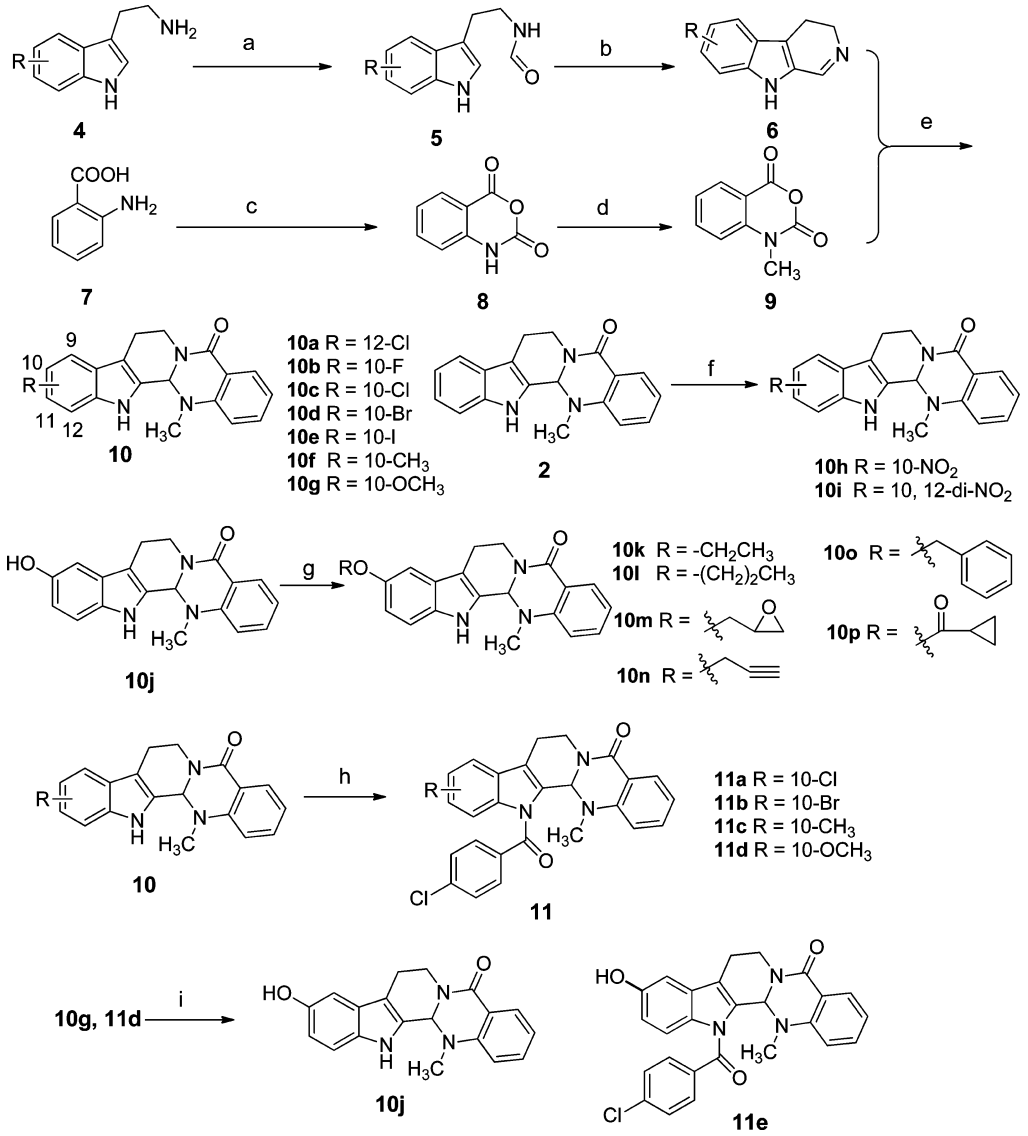

[a]Reagents and conditions: (a) ethyl formate, reflux, 6 h, yield 100%; (b) $POCl_3$, CH_2Cl_2, 0 °C, 6 h, yield 85.4−93.6%; (c) triphosgene, THF, reflux, 4 h, yield 95%; (d) CH_3I, KOH, DMF, 2 h, yield 87.4%; (e) CH_2Cl_2, rt, 12 h, yield 52.6−71.6%; (f) KNO_3, H_2SO_4, 0 °C, 12 h, yield 58.1−91.3%; (g) K_2CO_3, EtOH, reflux, 6 h, yield 76.3−88.8%; (h) 4-chlorobenzoyl chloride, NaH, DMF, 80 °C, 12 h, yield 28.9−52.1%; (i) BBr_3, CH_2Cl_2, −78 °C, 6 h, yield 58.3−63.2%.

synthesized by the oxidation of demethyl derivatives **25a−b**. Coupling of carboline **12** with 2-hydroxybenzoyl chloride (**27**) afforded the oxa- derivative **28**, which was subsequently acylated to compound **29**.

Two isomers of compound **18a** were synthesized by ruthenium(II)-catalyzed asymmetric transfer hydrogenation (Scheme 5).[46] The *β*-carboline intermediate **35** was prepared by reacting 4-(benzyloxy)aniline with ethyl 2-oxopiperidine-3-carboxylate, followed by treating with HCOOH. In the presence of $POCl_3$, *β*-carboline **35** was condensed with 5-fluoro-2-(methylamino)benzoate in dry THF to afford the dehydro derivative **37** in 50% yield. Using Noyori's procedure,[47] asymmetric reduction of **37** catalyzed by RuCl[(*S*,*S*)-Tsdpen]-(*p*-cymene) or RuCl[(*R*,*R*)-Tsdpen](*p*-cymene) gave (*S*)-**38** and (*R*)-**38**, respectively. Finally, after removal of the protection group, compounds (*S*)-**18a** and (*R*)-**18a** were obtained in 90% *ee*.

RESULTS AND DISCUSSION

A-Ring Modified Derivatives. Previously, the effects of N13 substitutions of compound **2** on the biological activities have been investigated.[45] Herein, SAR studies are mainly focused on introducing various substitutions on compound **2** or modifying its scaffold. First, a series of C10 and C12 substituted derivatives were synthesized. The growth inhibitory activities toward human cancer cell lines A549 (lung cancer), MDA-MB-435 (breast cancer), and HCT116 (colon cancer) were determined using MTT assay.[45] Compound **1**, TPT, and IRT were used as reference drugs. It can be seen that the type and position of the substitutions play an important role for the antiproliferative potency (Table 1). The 10-chloro derivative **10c** was inactive toward all the three cancer cell lines. When the chlorine atom of compound **10c** was replaced by other halogen atoms (i.e., fluorine, bromine, and iodine), improved antitumor activity was observed. The iodine atom (compound **10e**) seems

dx.doi.org/10.1021/jm300605m | J. Med. Chem. 2012, 55, 7593−7613

Scheme 2[a]

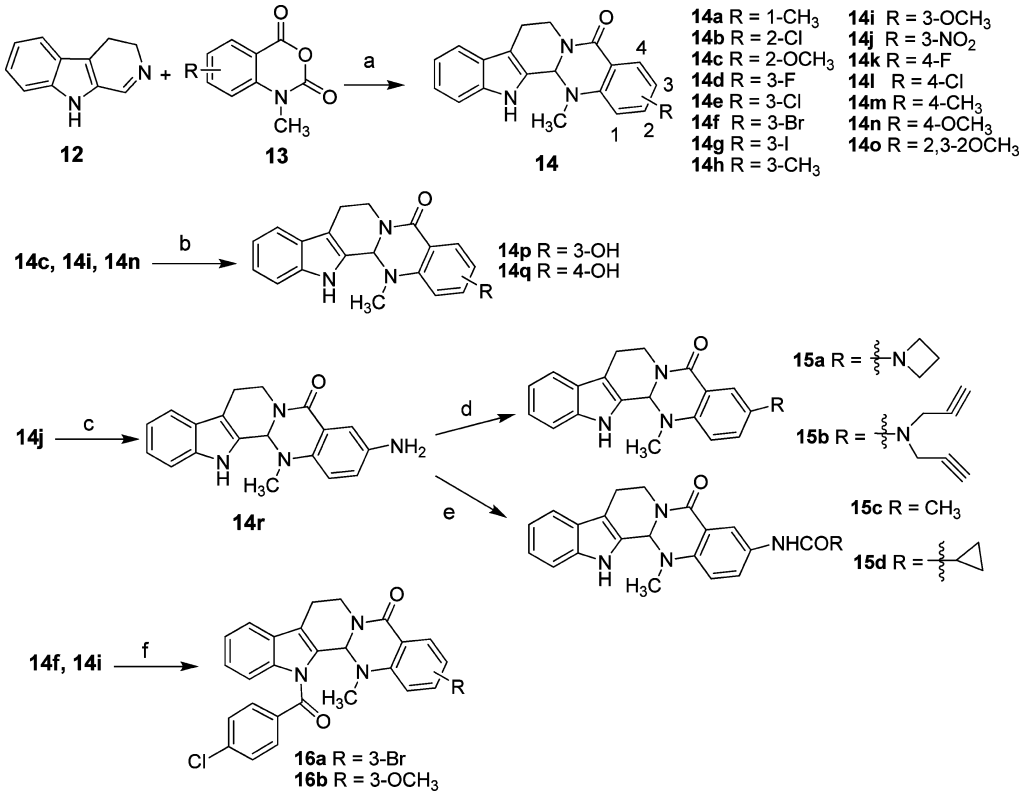

[a]Reagents and conditions: (a) CH_2Cl_2, 45 °C, 6 h, yield 13−87%; (b) BBr_3, CH_2Cl_2, −20 °C, 5 h, yield 50−52%; (c) 10% Pd/C, H_2, DMF, rt, 12 h, yield 73%; (d) 1,3-dibromopropane or 3-bromopropyne, K_2CO_3, DMSO, 60 °C, 7 h, yield 27−32%; (e) Ac_2O or cyclopropanecarbonyl chloride, Et_3N, CH_2Cl_2, rt, 2 h, yield 73−82%; (f) 4-chlorobenzoyl chloride, NaH, DMF, 80 °C, 8 h, yield 31−86%.

Scheme 3[a]

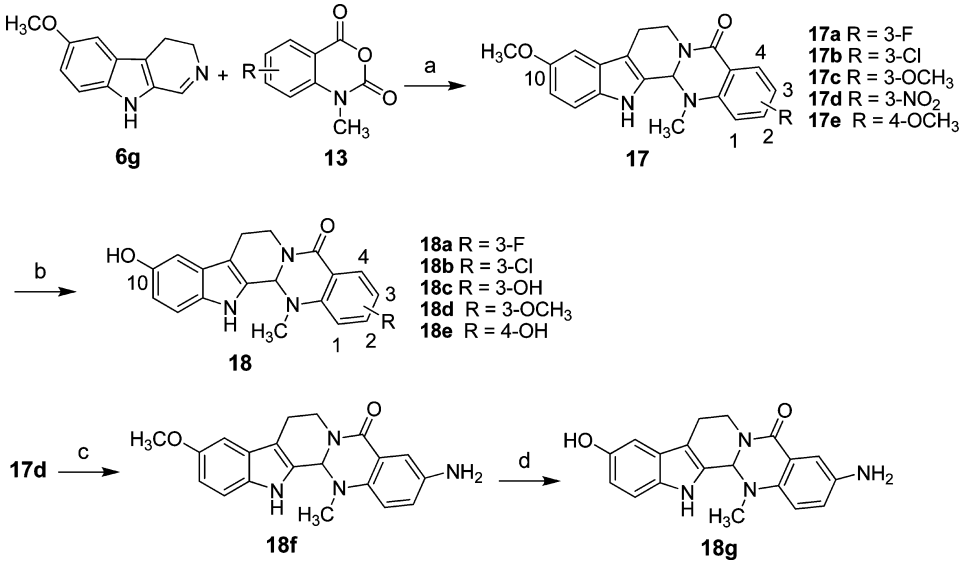

[a]Reagents and conditions: (a) CH_2Cl_2, 45 °C, 6 h, yield 45−91%; (b) BBr_3, CH_2Cl_2, −20 °C, 5 h, yield 31−63%; (c) 10% Pd/C, H_2, DMF, rt, 12 h, yield 79%; (d) BBr_3, CH_2Cl_2, −20 °C, 5 h, yield 31%.

to be the most favorable at C10. Compound **10e** showed higher antiproliferative activity (GI_{50} range: 0.26−11.39 μM) than reference drug **2** and IRT, but it was less potent than compound **1** and TPT. On the other hand, the movement of the chlorine atom from C10 (compound **10c**) to C12 (compound **10a**) led to the substantial increase of the antitumor activity. Compound **10a** showed excellent antiproliferative activity against MDA-MB-435 and HCT116 cancer cell lines with GI_{50} value lower than 0.003 μM, which was more active than all the reference drugs. The introduction of the nitro or methyl group on the C10 position of compound **2** resulted in two inactive derivatives (**10f** and **10h**).

dx.doi.org/10.1021/jm300605m | J. Med. Chem. 2012, 55, 7593−7613

Scheme 4[a]

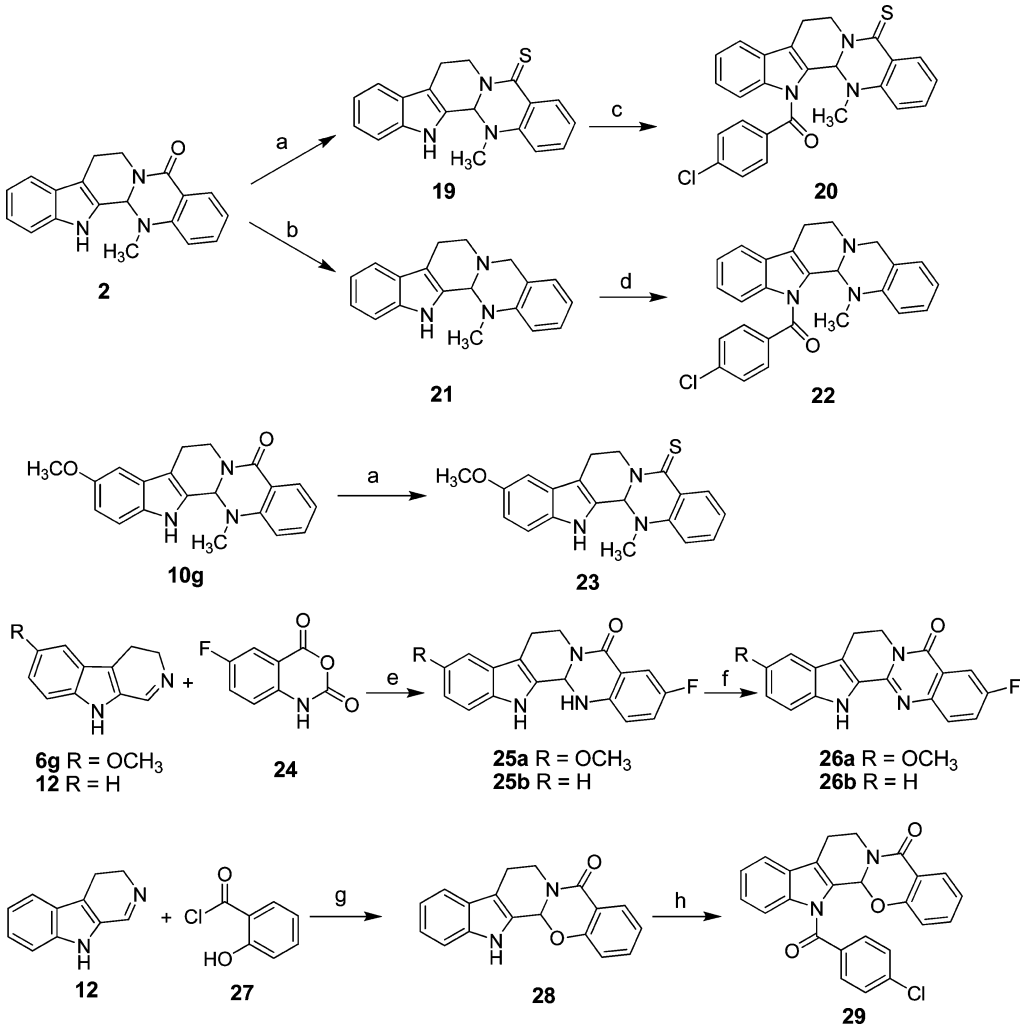

[a]Reagents and conditions: (a) Lawesson's reagent, PhMe, reflux, 6 h, 47.9−65.6%; (b) $LiAlH_4$, THF, rt, 12 h, yield 58.6%; (c) 4-chlorobenzoyl chloride, NaH, DMF, 80 °C,12 h, yield 69.5%; (d) 4-chlorobenzoyl chloride, NaH, DMF, 80 °C,12 h, yield 56.9%; (e) CH_2Cl_2, rt, 6 h, 78.5−84.1%; (f) IBX, DMSO, rt, 12 h, yield 86.7−89.9%; (g) CH_2Cl_2, rt, 12 h, yield 57.6%; h, 4-chlorobenzoyl chloride, NaH, DMF, 0 °C, 12 h, yield 57.2%.

The 10-nitro derivative **10h** can be activated by adding another nitro group on the C12 position. The dinitro derivative **10i** showed good activity against the MDA-MB-435 cell line (GI_{50} = 0.16 μM), but it was also inactive toward the other two cancer cell lines.

The most potent compound in this series is the 10-hydroxyl derivative **10j**, whose GI_{50} value was lower than 0.003 μM for all the three cancer cell lines. In contrast, the replacement of the C10 hydroxyl group by a methoxyl group (compound **10g**) led to significant decrease or loss of the antitumor activity. To further validate the importance of the hydroxyl group, a series of ether or ester derivatives **10k−p** were designed and synthesized. The in vitro antitumor assay revealed that all the ether derivatives showed decreased antiproliferative activity. Particularly, they almost lost the activity against the A549 cancer cell line. For the SAR of the substitutions on the hydroxyl group, the oxirane methyl group (compound **10m**) was relatively better than the ethyl (compound **10k**), propyl (compound **10l**), and allyl (compound **10n**) group. The benzyl substituted analogy **10p** was nearly inactive. In contrast, the ester derivative **10p** was more active than the ether analogues, especially for the activity against the HCT116 cell line.

In our previous studies, the 4-chloro-benzoyl group was found to be favorable for the N13 substitution.[45] In an attempt to investigate the synergistic effects of the A-ring and B-ring indole NH substitutions, C10 and N13 disubstituted derivatives **11a−e** were designed and synthesized. For some inactive or weakly active derivatives, such as compounds **10c**, **10d**, **10f** and **10h**, the addition of a 4-chloro-benzoyl group on the N13 atom resulted in improved antiproliferative activity and antitumor spectrum. For example, the 10-methyl derivative **10f** was inactive, whereas its corresponding C10 and N13 disubstituted derivative **11c** showed good antiproliferative activity against the MDA-MB-435 (GI_{50} = 1.14 μM) and HCT116 (GI_{50} = 11.4 μM) cell lines. For the highly active compound **10j**, the corresponding analogue **11e** showed comparable activity against the A549 cell line, but its potency against the other two cell lines was decreased.

E-Ring Modified Derivatives. 1-Methyl derivative (**14a**) showed potent in vitro antitumor activity, with GI_{50} values ranging from 0.011 to 0.23 μM (Table 2). When the C1 methyl group was moved to C3 (compound **14h**) or C4 (compound **14m**), the antiproliferative activity was decreased obviously. Introducing the substitutions on the C2 position led to the loss of the activity because two C2-substituted derivatives, **14b** and **14c**,

dx.doi.org/10.1021/jm300605m | J. Med. Chem. 2012, 55, 7593−7613

Scheme 5[a]

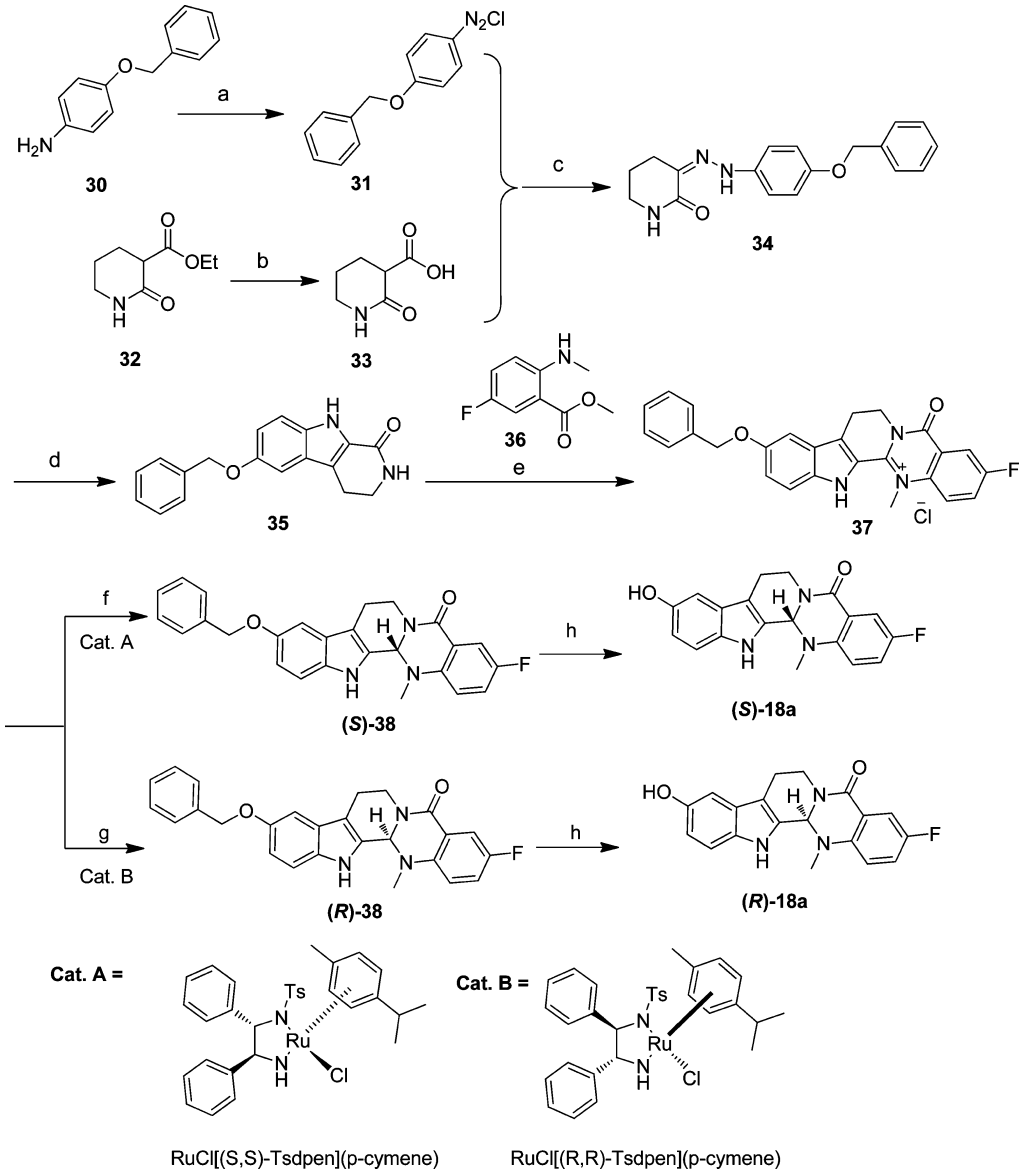

[a]Reagents and conditions: (a) $NaNO_2$, hydrochloric acid, H_2O, 0−5 °C, 2 h; (b) KOH, H_2O, rt, 12 h; (c) rt, 10 h; (d) HCOOH, reflux, 0.5 h, yield 59%; (e) $POCl_3$, THF, reflux, 3 days, yield 50%; (f) Cat. A, HCOOH:Et_3N (5:2), 0 °C, 8 h, yield 87%; (g) Cat. B, HCOOH:Et_3N (5:2), 0 °C, 8 h, yield 83%; (h) 10% Pd/C, H_2, DMF, rt, 12 h, yield 85−86%

were both inactive. In contrast, most of the C3-substituted derivatives, except for **14o** and **14j**, showed good antitumor activity. Among them, 3-fluoro (**14d**) and 3-chloro (**14e**) derivatives were the most active compounds in this series, with GI_{50} value lower than 0.003 μM for all the three cancer cell lines. For the other 3-halogen derivatives, the 3-bromo derivative **14f** showed moderate activity, whereas the 3-iodine derivative **14g** was almost inactive. When the C3 position was substituted by the methyl (compound **14h**) or methoxyl (compound **14i**) group, good antiproliferative activity was also observed for them, but they were less potent than the 3-fluoro or 3-chloro derivatives. As compared to the 3-substituted analogues, significantly decreased activity was observed for the corresponding 4-substituted derivatives (compounds **14k−n**).

Adding another methoxyl group on the C2 position of compound **14i** resulted in the decreased activity (compound **14o**). Interestingly, the replacement of the methoxyl group of **14i** and **14n** by a hydroxyl group (compounds **14p** and **14q**) led to significantly improved antitumor activity against the MDA-MB-435 and HCT116 cell lines. Particularly, the GI_{50} value of the 3-hydroxyl derivatives (**14p**) for the MDA-MB-435 cell line was lower than 0.003 μM. The 3-nitro derivative **14j** was inactive, but its reduced product **14r** showed potent activity against the MDA-MB-435 (GI_{50} = 0.15 μM) and HCT116 (GI_{50} = 8.92 μM) cell lines. When the amine group of compound **14r** was dialkylated, the corresponding compounds **15a** and **15b** showed increased activity against the HCT116 cell line. However, two amide derivatives **15c** and **15d** were only weakly active. Notably, all the amine and amide analogues were inactive again the A549 cell line. Compounds **16a** and **16b** were synthesized to evaluate the synergistic effects of the C3 and N13 substitutions. Unfortunately, the results were the reverse of the A-ring SAR. The additional 4-chloro-benzoyl group on the N13 position had negative effects on the antiproliferative activity.

dx.doi.org/10.1021/jm300605m | J. Med. Chem. 2012, 55, 7593−7613

Table 1. In Vitro Antitumor Activity of A-Ring Modified Evodiamine Derivatives (GI_{50}, μM)

compd	A549	MDA-MB-435	HCT116
10a	2.55 ± 0.17	<0.003	<0.003
10b	6.85 ± 0.41	27.35 ± 1.25	8.56 ± 0.63
10c	>200	>200	>200
10d	>200	37.57	>200
10e	11.39 ± 1.05	0.26 ± 0.03	0.78 ± 0.02
10f	>200	>200	>200
10g	>200	8.97 ± 0.52	>200
10h	>200	>200	>200
10i	>200	0.16 ± 0.01	>200
10j	<0.003	<0.003	<0.003
10k	>200	5.93 ± 0.23	19.17 ± 1.32
10l	>200	3.07 ± 0.10	8.05 ± 0.74
10m	48.88 ± 2.33	0.61 ± 0.03	2.98 ± 0.35
10n	>200	4.39 ± 0.25	13.96 ± 1.28
10o	>200	41.25	>200
10p	1.9 ± 0.04	0.08 ± 0.001	0.01 ± 0.002
11a	>200	72.72 ± 5.22	>200
11b	22.54 ± 1.62	38.73 ± 4.02	19.65 ± 0.86
11c	>200	1.14 ± 0.05	11.40 ± 0.98
11d	87.20 ± 5.20	11.83 ± 0.93	70.99 ± 6.11
11e	26.58 ± 1.09	<0.002	0.05 ± 0.002
1	0.17 ± 0.005	0.033 ± 0.003	0.083 ± 0.001
2	100 ± 9.60	20.20 ± 1.65	100 ± 7.23
TPT[a]	3.96 ± 0.64	0.034 ± 0.001	0.40 ± 0.02
IRT[b]	5.0 ± 0.05	12.2 ± 1.94	7.1 ± 0.25

[a]TPT = topotecan. [b]IRT = irinotecan.

Table 2. In Vitro Antitumor Activity of E-Ring Modified Evodiamine Derivatives (GI_{50}, μM)

compd	A549	MDA-MB-435	HCT116
14a	0.23 ± 0.015	0.084 ± 0.002	0.011 ± 0.001
14b	>200	>200	>200
14c	>200	>200	>200
14d	<0.003	<0.003	<0.003
14e	<0.003	<0.003	<0.003
14f	14.49 ± 1.06	1.50 ± 0.08	14.07 ± 1.04
14g	>200	2.94 ± 0.09	>200
14h	32.17 ± 2.89	0.32 ± 0.01	0.61 ± 0.03
14i	0.94 ± 0.01	0.29 ± 0.02	1.25 ± 0.05
14j	>200	>200	>200
14k	200 ± 15.36	42.60 ± 5.03	>200
14l	5.65 ± 0.25	1.43 ± 0.10	4.56 ± 0.18
14m	14.30 ± 1.03	20.20 ± 1.62	13.14 ± 0.68
14n	128.11 ± 15.20	22.26 ± 2.01	19.71 ± 1.32
14o	>200	8.97 ± 0.88	>200
14p	>200	<0.003	0.013 ± 0.000
14q	62.41 ± 5.65	0.24 ± 0.02	2.14 ± 0.24
14r	>200	0.15 ± 0.02	8.92 ± 0.95
15a	>200	0.20 ± 0.01	3.85 ± 0.29
15b	>200	2.03 ± 0.12	0.21 ± 0.01
15c	>200	59.15 ± 4.23	70.50 ± 6.00
15d	>200	>200	186.57 ± 23.65
16a	>200	8.72 ± 0.55	39.71 ± 0.33
16b	>200	184.39 ± 12.29	88.68 ± 5.84

Synergistic Effects of A-Ring and E-Ring Modifications. The results of A-ring SAR indicated that the C3 hydroxyl group is important for the antitumor activity. On the other hand, the introduction of a C3-fluoro, chloro, or hydroxyl group on the E-ring also led to substantial increase of the antiproliferative activity. In an attempt to investigate their synergistic effects with E-ring, disubstituted analogues **17a−e** and **18a−g** were synthesized by combing the favorable substitutions of the A- and E- ring. It can be seen that all the hydroxyl derivatives are more active than their corresponding methoxyl analogues (Table 3). The results were consistent with A- and E-ring SAR,

Table 3. In Vitro Antitumor Activity of A-Ring and E-Ring Disubstituted Evodiamine Derivatives (GI_{50}, μM)

compd	A549	MDA-MB-435	HCT116
17a	200 ± 13.68	<0.003	0.78 ± 0.05
17b	13 ± 1.03	2.0 ± 0.06	0.004 ± 0.000
17c	>200	9.8 ± 0.67	0.033 ± 0.001
17d	>200	>200	0.15 ± 0.02
17e	98 ± 5.87	21 ± 1.29	42 ± 3.02
18a	<0.003	<0.003	<0.003
18b	0.12 ± 0.005	0.005 ± 0.000	0.005 ± 0.000
18c	0.75 ± 0.04	0.003 ± 0.000	0.007 ± 0.000
18d	1.6 ± 0.08	0.66 ± 0.04	0.07 ± 0.001
18e	0.23 ± 0.02	0.013 ± 0.001	0.009 ± 0.000
18f	62 ± 5.25	12 ± 1.03	6.6 ± 0.50
18g	4.0 ± 0.13	0.076 ± 0.006	0.007 ± 0.000

which further highlighted the importance of hydroxyl group for the antitumor activity. In addition, excellent antiproliferative activity was retained after the combination of A-ring and E-ring substitutions. Highly active compounds **18a−c**, **18e**, and **18g** were more potent than the reference drugs. For example, the GI_{50} value of the 3-fluoro-10-hydroxyl derivative (**18a**) was lower than 0.003 μM against all the three cancer cell lines. Compounds **18b**, **18c**, **18e**, and **18g** were more selective to the MDA-MB-435 and HCT116 cell lines with GI_{50} values in low nanomolar range. More importantly, after introducing one or two hydrophilic groups (i.e., OH and NH_2) on the scaffold of compound **2**, the water solubility can be significantly improved, which is very helpful for their in vivo antitumor efficacy.

D-Ring Modified Derivatives. Unlike the structural optimization of A-ring and E-ring, the investigation of D-ring SAR was mainly focused on the modification of the scaffold. First, the C5 carbonyl group of compound **2** was replaced by a thiocarbonyl group (compound **19**) or reduced to the methylene group (compound **21**). As compared to compound **2**, the thiocarbonyl derivative **19** showed improved antiproliferative activity against all the three cancer cell lines (GI_{50} range: 12.24−90.73 μM). To validate the positive effect of the thiocarbonyl group, compound **23** was synthesized and evaluated. Similarly, the thiocarbonyl derivative **23** was more active than the corresponding carbonyl analogue **10g**. On the other hand, the antitumor activity of the reduced product **21** was similar to that of compound **2**. Unfortunately, the addition of the 4-chlorobenzoyl group on the N13 position of compounds **19** and **21** led to nearly loss of the activity. The SAR results are reverse to those of compound **2**, indicating that there might be different SARs when the scaffold of compound **2** was changed. Second, the SAR of the N14 methyl group was investigated. Two N14 demethyl derivatives, **25a** and **25b**, were synthesized, which showed decreased activities. When the free amine group of compounds **25a−b** was oxidized to the enamine group (**26a−b**), namely changing the scaffold of compound **2** to rutaecarpine,[48] their antiproliferative activity was still lower than the corresponding

dx.doi.org/10.1021/jm300605m | J. Med. Chem. 2012, 55, 7593−7613

Table 4. In Vitro Antitumor Activity of D-Ring Modified Evodiamine Derivatives (GI_{50}, μM)

compd	A549	MDA-MB-435	HCT116
19	90.73 ± 8.09	12.24 ± 1.26	46.49 ± 3.88
20	>200	>200	>200
21	>200	16.17 ± 1.24	>200
22	>200	95.95 ± 2.66	>200
23	106.17 ± 9.67	3.69 ± 0.23	21.38 ± 1.08
25a	60.12 ± 3.22	18.50 ± 0.96	26.71 ± 1.77
25b	>200	>200	>200
26a	>200	>200	137.7 ± 10.05
26b	47.2 ± 3.02	15.9 ± 1.44	20.0 ± 1.76
28	2.40 ± 0.12	3.13 ± 0.20	3.03 ± 0.15
29	>200	>200	>200

derivatives of compound **2** (Table 4). Third, the N14-methyl group of compound **2** was replaced by the oxygen atom to afford a new scaffold (oxa-evodiamine). Interestingly, compound **28** was far more potent than compound **2** with GI_{50} values in the range of 2.4−3.13 μM. However, its N13 substituted derivative **29** was inactive. The result further validated the fact that different D-ring scaffolds resulted in different SAR for the N13 position.

Effect of C13b Chirality on the Antitumor Activity. Compound **2** and its derivatives have an asymmetric center at the C13b position (Figure 1). The effect of C13b chirality on the antitumor activity was investigated for the first time. Both *R*- and *S*- isomers of compound **18a**, a highly active derivative, were synthesized by asymmetric transfer hydrogenation. To obtain robust results, their antiproliferative activity was evaluated for five kinds of human cancer cell lines. As shown in Table 5, the C13b chirality showed distinct effects toward different cell lines. For the A549 and HCT116 cell lines, (*S*)-**18a** was slightly more active than the *R*-isomer. Significant difference of the activity was observed for the ZR-75−30 (human breast cancer) and KYSE (human esophageal squamous cell carcinoma) cell lines; the *S*-isomer was about 580-fold more potent than the *R*-isomer. However, there was reverse trend for the CNE cell line (human thyroid carcinoma) and (*R*)-**18a** showed slightly higher activity than the *S*-isomer.

Summary of the SARs. Summary of the SARs is depicted in Figure 2. First, the introduction of the proper substitution on the scaffold of compound **2** can led to substantial improvement of the antitumor activity. Positions C1, C3, C10, and C12 are favorable to be substituted. Fluorine is favored at the C3 position, while chlorine is suitable for both C3 and C10 position. It should be noted that the free hydroxyl group is important for the excellent antiproliferative potency. Second, the modification of D-ring scaffold is tolerated. The transformation of the C5 carbonyl to the thiocarbonyl group or changing the N14-methyl group to an oxygen atom has positive effects on the antitumor activity. Third, there are synergistic effects for the C3 and C10 substitutions. Compounds **18a−c** and **18g**, bearing one or two hydrophilic groups, not only showed excellent antitumor activity but also possess good water solubility, which were subjected to the evaluation of in vivo antitumor efficacy.

Antitumor Spectrum of the Selected Derivatives. From the above results, a number of derivatives of compound **2** were found to be highly potent against A549, HCT116, and MDA-MB-435 cell lines. To evaluate their antiproliferative effects in a broader manner, the activity of compounds **10a**, **14d**, and **18a** were tested against a variety of human cancer cell lines including U20S (osteosarcoma), PANC-1 (prostate carcinoma), HepG2 (liver cancer), PC-3 (pancreatic cancer), HL-60 (acute myeloblastic leukemia), and Saos-2 (osteogenic sarcoma). As depicted in Table 6, the tested compounds showed broad antitumor spectrum. They are particularly effective against the HL-60 cell line with GI_{50} values lower than 3 nM. They also showed moderate to good antiproliferative activity against the PANC-1, HepG2, and PC-3 cell lines. Notably, compound **18a** showed remarkably higher activity against the PANC-1 cell line (GI_{50} < 3 nM) than compound **1** (GI_{50} = 6.29 μM). With the exception of compound **14d**, the other compounds including the

Table 5. In Vitro Antitumor Activity of the Isomers of Compound 18a (GI_{50}, μM)

isomers	A549	HCT116	ZR-75-30	CNE	KYSE-150
(*R*)-**18a**	0.0046 ± 0.000	0.011 ± 0.000	1.75 ± 0.09	5.88 ± 0.42	1.23 ± 0.10
(*S*)-**18a**	0.0037 ± 0.000	0.0036 ± 0.000	0.003 ± 0.000	8.11 ± 0.79	0.003 ± 0.000

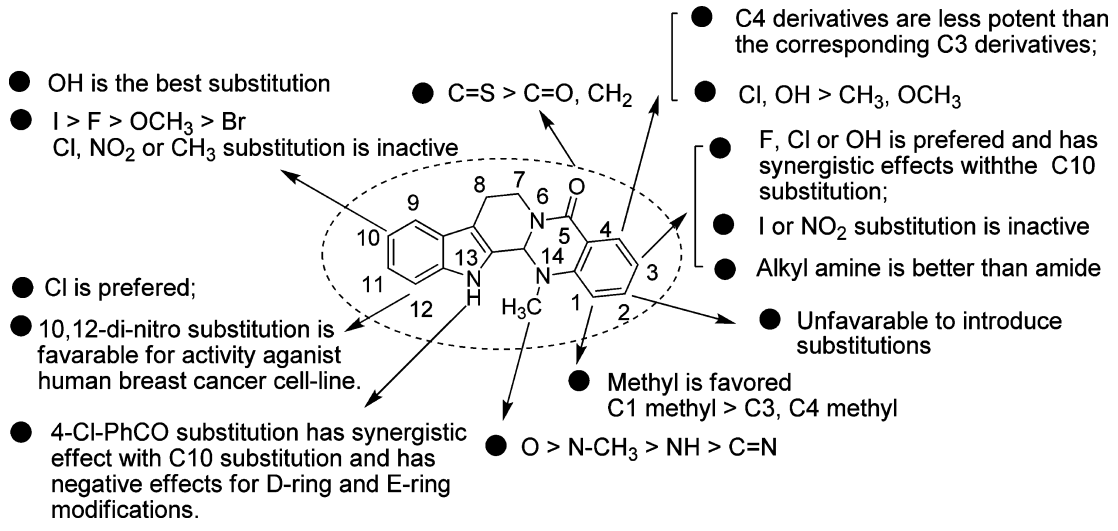

Figure 2. Summary of the structure−activity relationships of the evodiamine derivatives.

dx.doi.org/10.1021/jm300605m | *J. Med. Chem.* 2012, 55, 7593−7613

Table 6. In Vitro Antitumor Spectrum of Selected Evodiamine Derivatives (GI_{50}, μM)

compd	U20S	PANC-1	HepG2	PC-3	HL-60	Saos-2
10a	>296	0.12 ± 0.01	2.31 ± 0.13	>296	<0.003	>296
14d	129 ± 10.23	1.70 ± 0.09	188 ± 12.55	34.2 ± 2.85	<0.003	205 ± 16.02
18a	>296	<0.003	23.8 ± 1.65	92.3 ± 6.77	<0.003	>296
1	>287	6.29 ± 0.50	0.22 ± 0.006	>287	<0.003	>287

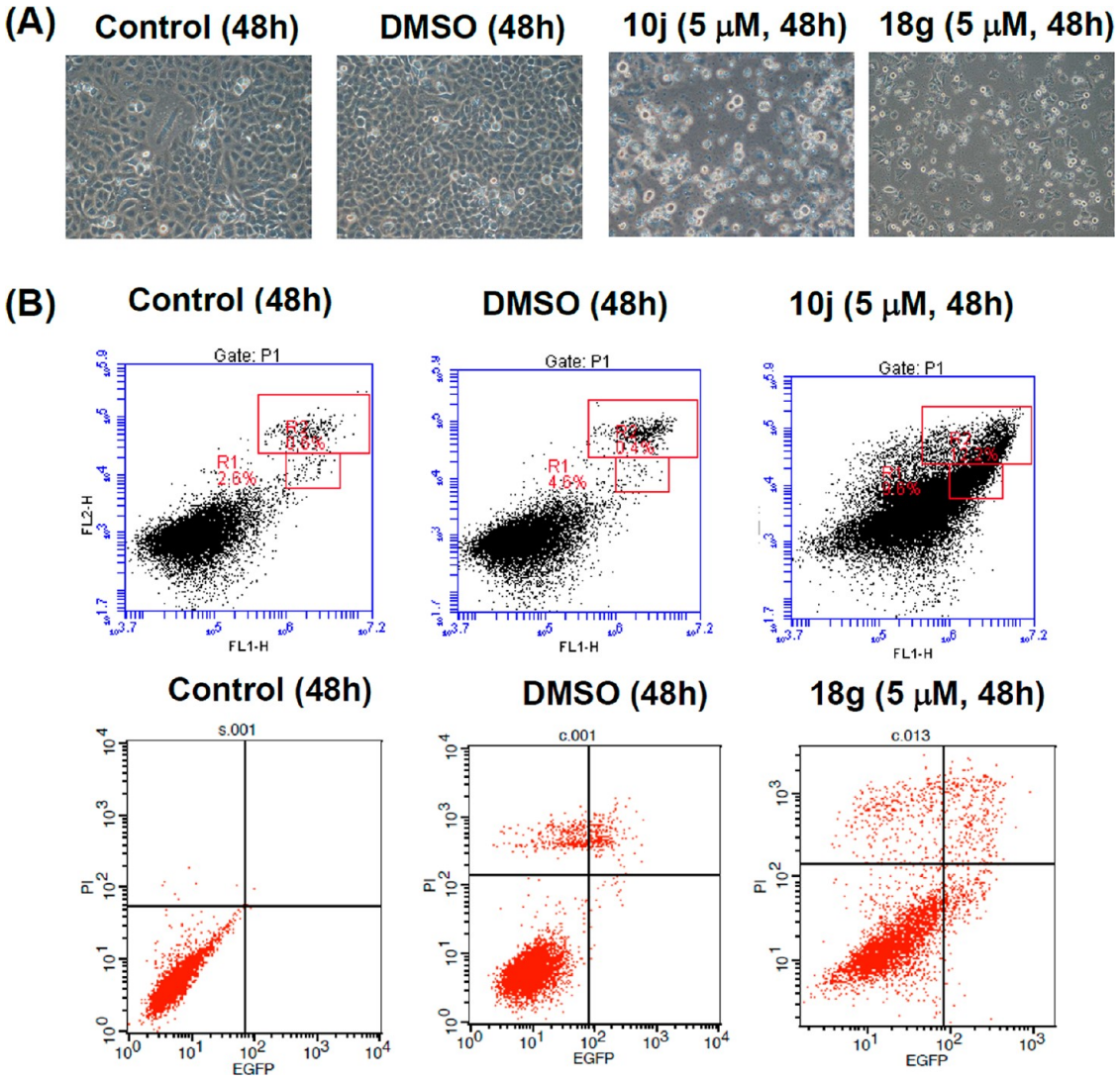

Figure 3. (A) The effect of evodiamine derivatives on human cancer cell morphology. A549 cells were treated with DMSO and 5 μM of compounds **10j** and **18g** for 48 h, and representative photographs were captured under a light microscope. (B) Evodiamine derivatives-induced cell apoptosis. A549 cells were treated with DMSO and 5 μM of compounds **10j** and **18g** for 48 h. Apoptosis was examined by flow cytometry ($n = 3$). Representative photographs from three independent experiments were displayed.

reference drug **1** were inactive against the U20S and Saos-2 cell lines.

The Effect of Selected Derivatives on Apoptosis in A549 Cells. The effect of selected derivatives of compound **2**, namely compounds **10j** and **18g**, on the induction of apoptosis was also evaluated by cell morphology (Figure 3A) and fluorescence-activated cell sorting (Figure 3B). The in vitro morphological changes of the cells treated with selected derivatives were examined. Visual assessment of the immunostaining suggested that the majority of A549 cells became small, round, and floating after the treatment with 5 μM of various derivatives for 48 h. In contrast, the untreated control group and DMSO group displayed a normal shape and well-ordered cytoskeleton under the same conditions. Moreover, the effects of several active derivatives on the induction of apoptosis in A549 cells were evaluated by flow cytometry. The percentage of apoptotic cells in the control group and DMSO group at 48 h was 0.47% and 0.43%, respectively. After treating with 5 μM of compounds for 48 h, the percentage of apoptotic cells for compounds **10j** and **18g** was 13.07% and 14.48%, respectively, suggesting that they showed remarkable apoptotic effect.

Top1 Inhibitory Activity and the Binding Modes. Previously, Top1 was identified as a target of compound **2** and its derivatives. They act by stabilizing a covalent Top1−DNA complex called the cleavable complex.[45] Herein, Top1-mediated DNA cleavage assays with purified Top1 were used to investigate

dx.doi.org/10.1021/jm300605m | J. Med. Chem. 2012, 55, 7593−7613

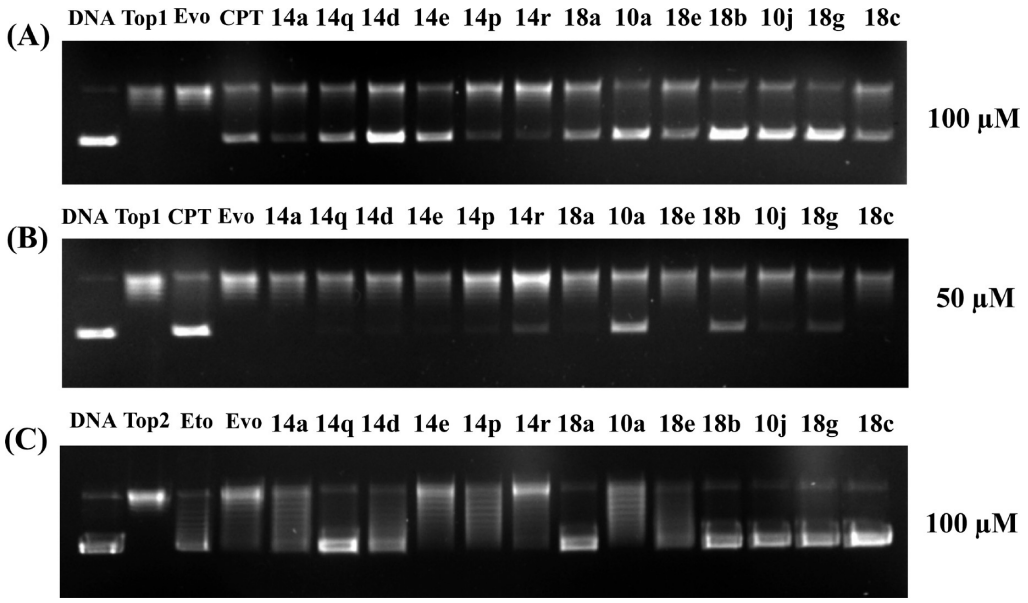

Figure 4. Top1 and Top2 inhibitory activity of the evodiamine derivatives. (A) Inhibition of Top1 relaxation activity at 100 μM. Lane 1, supercoiled plasmid DNA; lane 2, DNA + Top1; lane 3, DNA + Top1 + evodiamine; lane 4, DNA + Top1 + compound **1**; lanes 5−17, DNA + Top1 + evodiamine derivatives (**14a**, **14q**, **14d**, **14e**, **14p**, **14r**, **18a**, **10a**, **18e**, **18b**, **10j**, **18g**, and **18c**, respectively). (B) Inhibition of Top1 relaxation activity at 50 μM. The lanes are the same as the assay at 100 μM. (C) Inhibition of Top2 relaxation activity at 50 μM. Lane 1, supercoiled plasmid DNA; lane 2, DNA + Top2; lane 3, DNA + Top2 + etoposide; lane 4, DNA + Top2 + evodiamine; lanes 5−17, DNA + Top2 + evodiamine derivatives.

the inhibitory activity of representative compounds with high activity (i.e., compounds **10a**, **10j**, **14a**, **14d**, **14e**, **14p**, **14q**, **14r**, **18a**, **18b**, **18c**, **18e**, and **18g**). Top1 and supercoilded DNA pBR322 were incubated in the presence of the test compounds, whose ability to stabilize the cleavable complex were evaluated by the appearance of short DNA fragments. As shown in Figure 4A, all the tested compounds were found to be active against Top1-mediated relaxation of supercoiled DNA at the concentration of 100 μM. All of them showed higher inhibitory activity than compound **2**, which was only active at the concentration of 500 μM. We further tested the Top1 inhibitory activity at the concentration of 50 μM, and four compounds, namely **10a**, **18b**, **10e**, and **18g**, retained inhibitory activity (Figure 4B). Notably, the tested compounds were less active than compound **1**, but they showed comparable or better antiproliferative activities, suggesting that there might be additional targets for them.

Next, the binding modes of compounds **10j**, **18e**, **18g**, and **18c** were investigated by molecular docking and molecular dynamics (MD) simulations. All of these compounds bear one or two hydroxyl group on ring A or ring E, and thus the function of these hydroxyl groups can be investigated. GOLD 5.0.1[49] and Desmond,[50] with previously established protocols,[45] were used for computer modeling. As depicted in Figure 5, the binding poses of the derivatives were similar to that of compound **2**. Their indole ring intercalated at the site of DNA cleavage and formed base-stacking interactions with both the −1 (upstream) and +1 (downstream) base pairs. However, unlike compound **2**, its derivatives formed different hydrogen bonding interactions with the active site of Top1. Previously, the indole NH of compound **2** was found to form a hydrogen bond with Arg364.[45] For the hydroxyl derivatives, their indole NH was deviated from Arg364. Instead, the oxygen atom of A-ring hydroxyl group formed hydrogen bonding interaction with Arg364. Notably, the D-ring carbonyl oxygen atom formed an additional hydrogen bond with Asn352. However, no direct interaction between E-ring hydroxyl or amine group and Top1 was observed.

Discovery of Evodiamine Derivatives as Dual Top1/Top2 Inhibitors by in Silico Target Identification. The results of Top1 assay indicated that the antiproliferative activity of the tested derivatives did not correlate well with their Top1 inhibitory. It is inferred that there might be additional targets for them. To validate the hypothesis, ChemMapper,[51,52] a free web server for computational target identification, was used to predict the potential targets for the highly potent compound **14d**. ChemMapper is based on the concept that compounds sharing high 3D similarities may have relatively similar target association profile. ChemMapper performs the 3D similarity searching, ranking, and superposition by combining the strength of molecular shape superposition and chemical feature matching. After searching the MDDR database,[53] a list of potential targets was identified (see Table S1 in Supporting Information). Interestingly, topoisomerase II (Top2), a well-known antitumor target, was found to be ranked the fourth in the list. Top2 exists in two isoforms, α (alpha) and β (beta), and Top2α is commonly used for assaying.[54] Thus, the Top2α inhibitory activity of compound **14d** was determined in a relaxation assay.[55] As shown in Figure 4C, compound **14d** was proven to be a potent inhibitor of the catalytic activity of Top2. Particularly, it was more active than the well-known Top2α inhibitor etoposide (for relative Top2α inhibition rate, see Table S2 in Supporting Information). Moreover, compound **14d** was observed to be competitive binding with ATP and the increase of the ATP concentration resulted in the loss of the inhibitory activity of compound **14d**. Inspired by the results, other highly potent compounds were also assayed for their Top2α inhibitory activity (Figure 4C). To our delight, most of the tested compounds showed moderate to good Top2α inhibitory activity, except for compounds **10a**, **14e**, and **14p**. Besides compound **14d**, derivatives **14q**, **18a**, **18b**, **10j**, **18f**, and **18c** also showed better activity than etoposide. The above results indicated that compound **2** and its derivatives are dual inhibitors of Top1 and Top2. As compared to compound **2**, the significant increase of the antitumor activities for its derivatives

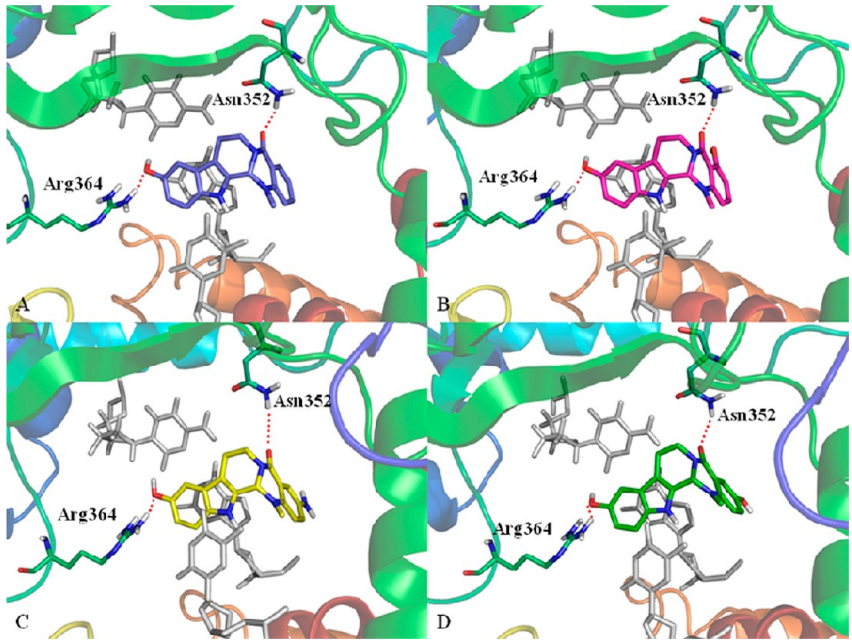

Figure 5. Schematic representation of the proposed binding mode for compounds **10j** (A), **18e** (B), **18g** (C), and **18c** (D) in the Top1−DNA complex. The figure was generated using PyMol (http://www.pymol.org/).

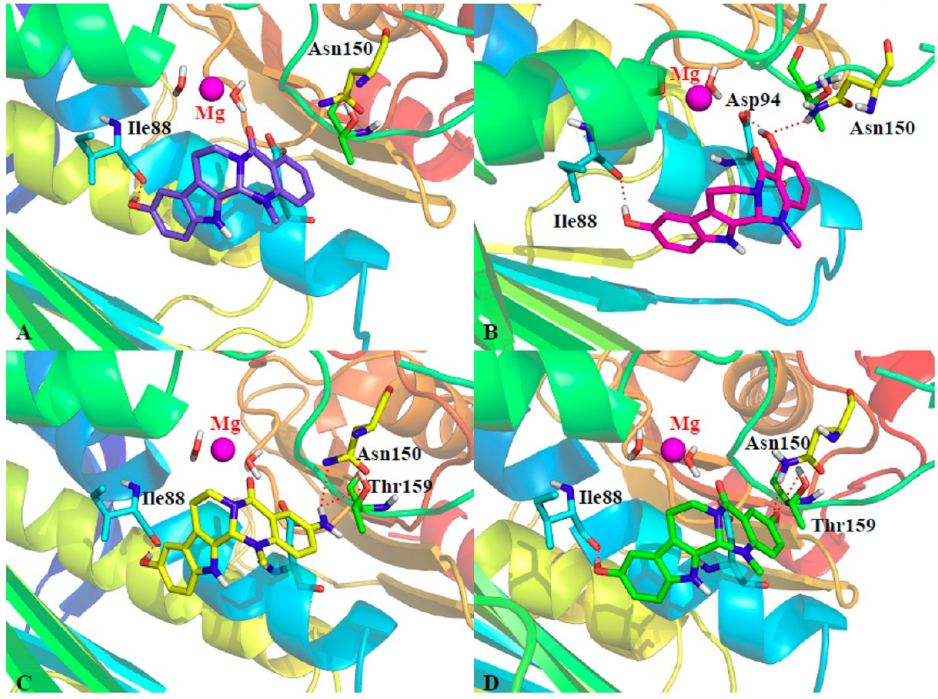

Figure 6. Schematic representation of the proposed binding mode for compounds **10j** (A), **18e** (B), **18g** (C), and **18c** (D) in the ATP-binding domain of Top2α. The figure was generated using PyMol (http://www.pymol.org/).

may be due to their improved inhibitory activity toward both Top1 and Top2.

To investigate the interactions between the tested compounds and Top2α, compounds **10j**, **18e**, **18g**, and **18c** were subjected to molecular docking and molecular simulations. They were observed to be well-fitted into the ATP-binding domain of Top2α (Figure 6). The A-ring C10 hydroxyl group formed a hydrogen bond with the backbone amide of Ile88. Interestingly, the E-ring hydroxyl or amine group that did not directly interact with Top1 formed hydrogen bonding interactions with the surrounding residues. For compound **18e**, its C4 hydroxyl group formed two hydrogen bonds with Asp94 and Asn150, respectively. For compounds **18g** and **18c**, hydrogen bonding interaction was observed between its C3 amine or hydroxyl group with Asn150 and Thr159. The docking model was consistent with the fact that E-ring hydroxyl or amine was important for the activity.

DNA Binding Properties. Interaction of the compounds with DNA induces both hypochromic and bathochromic shifts in the absorption spectrum.[56] The interaction of compounds **10j**,

dx.doi.org/10.1021/jm300605m | J. Med. Chem. 2012, 55, 7593−7613

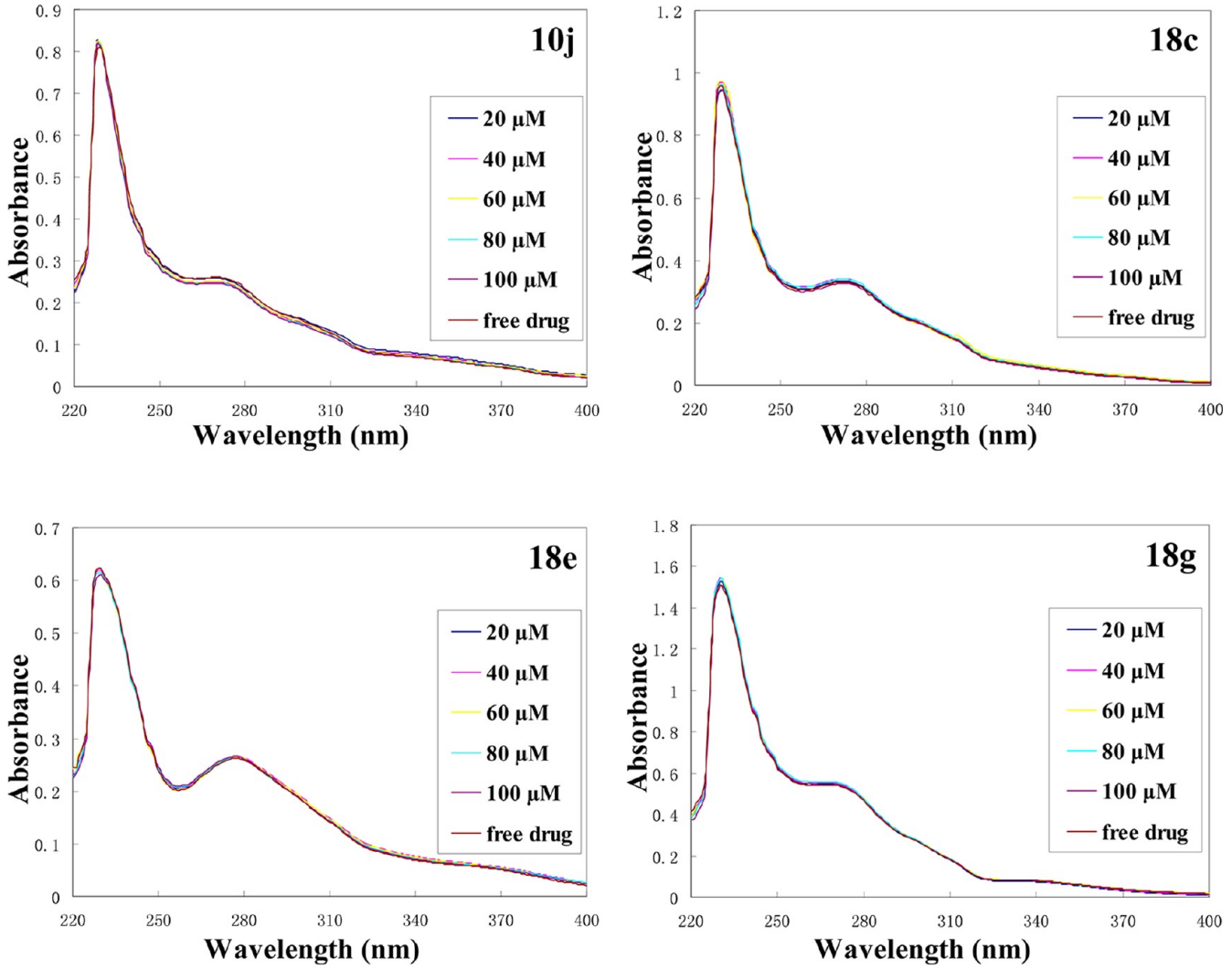

Figure 7. UV/vis absorption spectra of compounds **10j**, **18c**, **18e**, and **18g** (50 μM) alone (free drug lines) or with increasing concentrations of ct-DNA from 20 to 100 μM, respectively.

18c, **18e**, and **18g** with calf thymus DNA (ct-DNA) were examined by absorbance titration experiments (Figure 7). As DNA concentration was increased, both hypochromic and bathochromic shifts were not observed in these experiments. It was concluded that these compounds could not bind to the DNA. To further prove our conclusion, Top1 unwinding assay and Hoechst 33258 displacement experiments were performed to test whether these compounds could intercalate into DNA or bind to the minor groove of DNA. A negatively supercoiled pBR322 DNA was relaxed by an excess amount of Top1 in the present of the test compounds. Then, the compounds were removed by phenol extraction. If the compound is an intercalator, such as ethidium bromide, the intercalation of the compound between DNA base pairs induces a positively supercoiled DNA.[57] As shown in Figure 8, the intercalator ethidium bromide induced a supercoiled DNA following Top1 treatment. However, DNA remained relaxed in the present of **10j**, **18c**, **18e**, and **18g**, indicating that they were not DNA intercalators. The fluorescence of the groove binder Hoechst 33258 increases by 140-fold upon DNA binding.[58,59] So the displacement of Hoechst 33258 could be monitored by a decrease in the fluorescence intension.[60,61] As the test compounds concentration was increased, the fluorescence intension remained unchanged, indicating that compounds **10j**, **18c**, **18e**, and **18g** failed to bind to the minor groove of DNA (Supporting Information).

Mechanism of Top1 and Top2 Inhibition. Both Top1 and Top2 inhibitors were classified into two categories, poisons and catalytic inhibitors. Top1 poison, such as CPT, could stabilize the Top1−DNA cleavage complex and increase the intensity of nicked band in the EtBr containing gel. Compared with CPT, compounds **10j**, **18c**, **18e**, and **18g** could also increase the intensity of nicked band (Figure 9A), indicating these compounds were Top1 poisons. Top2 poisons, including etoposide and doxorubicin, act by stabilizing Top2−DNA cleavage complex and lead to the formation of a new DNA band corresponding to linear plasmid DNA. In contrast to etoposide, no linear plasmid DNA was detected in the case of test compounds (**10j**, **18c**, **18e**, and **18g**, Figure 9B). This result suggested that these compounds did not stabilize the Top2−DNA cleavage complex. It was concluded that these compounds acted as Top2 catalytic inhibitors rather than Top2 poisons.

Inhibition of the Tumor Growth of A549 and HCT116 Tumor Xenografts in Nude Mice. To investigate the in vivo effects of the synthesized compounds on tumor growth, two xenograft models were prepared by inoculating human lung cancer A549 or human colon cancer HCT116 cells on the nude

dx.doi.org/10.1021/jm300605m | J. Med. Chem. 2012, 55, 7593−7613

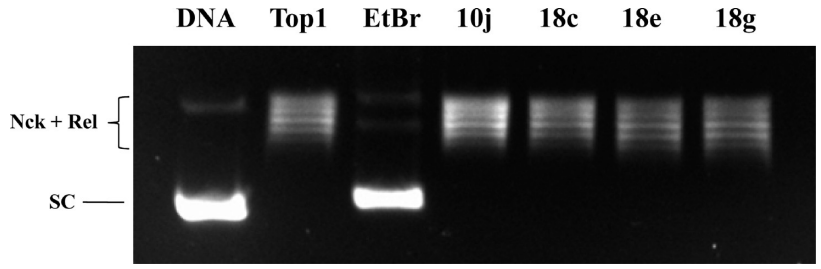

Figure 8. Investigation of the intercalating ability of the evodiamine derivatives based on Top1 unwinding assay. Lane 1, supercoiled plasmid DNA (pBR322); lane 2, DNA + Top1; lane 3, DNA + Top1 + EtBr (1 μg/mL); lanes 4−7, DNA + Top1 + evodiamine derivatives (**10j**, **18c**, **18e**, and **18g** at 100 μM, respectively). The position of nicked DNA (Nck), relaxed DNA (Rel), and supercoiled pBR322 (SC) was indicated.

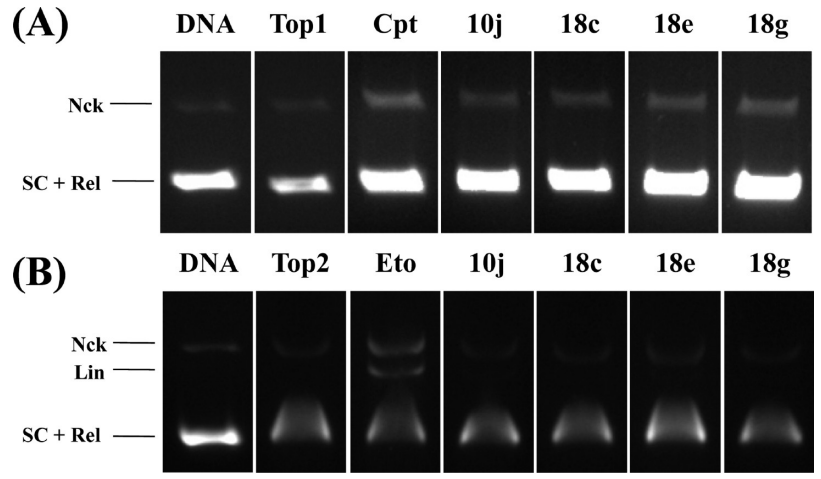

Figure 9. Top1 and Top2 DNA cleavage gels of the evodiamine derivatives. (A) Top1-mediated DNA cleavage assay gel of test compounds using supercoiled pUC19. Lane 1, supercoiled plasmid DNA (pUC19); lane 2, DNA + Top1; lane 3, DNA + Top1 + compound **1** (100 μM); lanes 4−7, DNA + Top1 + evodiamine derivatives (**10j**, **18c**, **18e**, and **18g** at 100 μM, respectively). (B) Top2-mediated DNA cleavage assay gel of test compounds using supercoiled pBR322. Lane 1, supercoiled plasmid DNA (pBR322); lane 2, DNA + Top2; lane 3, DNA + Top2 + etoposide (100 μM); lanes 4−7, DNA + Top2 + evodiamine derivatives (**10j**, **18c**, **18e**, and **18g** at 100 μM, respectively). The position of nicked DNA (Nck), liner DNA (Lin), relaxed DNA (Rel), and supercoiled DNA (SC) was indicated.

mice. Because the in vivo antitumor potency usually does not correlate well with their in vitro antiproliferative activities, representative compounds were selected to evaluate their potency in the two xenograft models. The compounds for in vivo testing were chosen according to their chemical structures and antitumor activity. Initially, compounds **10j** and **14d** were tested in the A549 xenograft model at the dose of 1 mg/kg. As shown in Figure 10A, intraperitoneal (ip) injection of the two compounds for 13 days significantly inhibited tumor growth ($p < 0.05$). Next, the dose of compounds **14e** and **18a** were doubled (2 mg/kg), but no improvement of the tumor growth inhibition was observed (Figure 10B). Meanwhile, all the compounds were found to be well tolerated during the test and showed no significant loss of body weight, suggesting that the toxicity of them is low. Among them, the 10-hydroxyl derivative **10j** showed the best in vivo potency. In the HCT116 xenograft model, all the tested compounds (i.e., **10a**, **10j**, **18a**, **18b**, **18c**, and **18g**) also showed significant inhibitory effects on the tumor growth at the dose of 2 mg/kg (Figure 10C). Except for compounds **10a**, **18b**, and **18c**, body weight of the nude mice was not significantly affected during the test (see Figure S1 in Supporting Information). As compared to compound **10j**, its 3-chloro derivative **18b** showed increased in vivo potency, whereas the potency of its 3-fluoro derivative **18a** was decreased. The highest in vivo antitumor potency was observed for 3-amino-10-hydroxyl evodimine (**18g**).

The Requirements and Advantages of Dual Top1/Top2 Inhibitors. Topoisomerases are validated antitumor targets that act as complex molecular engines to modulate DNA topology and maintain chromosome superstructure and integrity.[62] Top1 or Top2 inhibitors show outstanding antitumor efficacy, which form the basis of many cancer chemotherapeutic protocols. Despite decades of study, the investigation of new biological functions of topoisomerases as therapeutic targets and also the development of novel inhibitors remains highly active.[62−64] The available evidence suggests that the therapeutic potential of topoisomerase is far from exhausted.[64] For many forms of malignant tumors, potent cytotoxic agents, such as topoisomerase inhibitors, are frequently used as the only remedy to limit rapid tumor growth, progression, and metastasis. Moreover, topoisomerase inhibitors can be essentially used in combination with targeted therapeutic agents, such as kinase inhibitors, especially for the treatment of advanced solid tumors. However, current Top1 or Top2 inhibitors have two major limitations: toxicity and drug resistance. In this scenario, the development of dual Top1/Top2 inhibitors represents a promising approach to overcome the drawbacks of single inhibitors.[65,66] Dual Top1/Top2 inhibitors have several advantages as novel antitumor agents. Given that both Top1 and Top2 are well-qualified antitumor targets and have overlapping functions in DNA metabolism, targeting both Top1 and Top2 could increase overall antitumor activity with reduced toxic side effects.[67] On the other hand, the

dx.doi.org/10.1021/jm300605m | J. Med. Chem. 2012, 55, 7593−7613

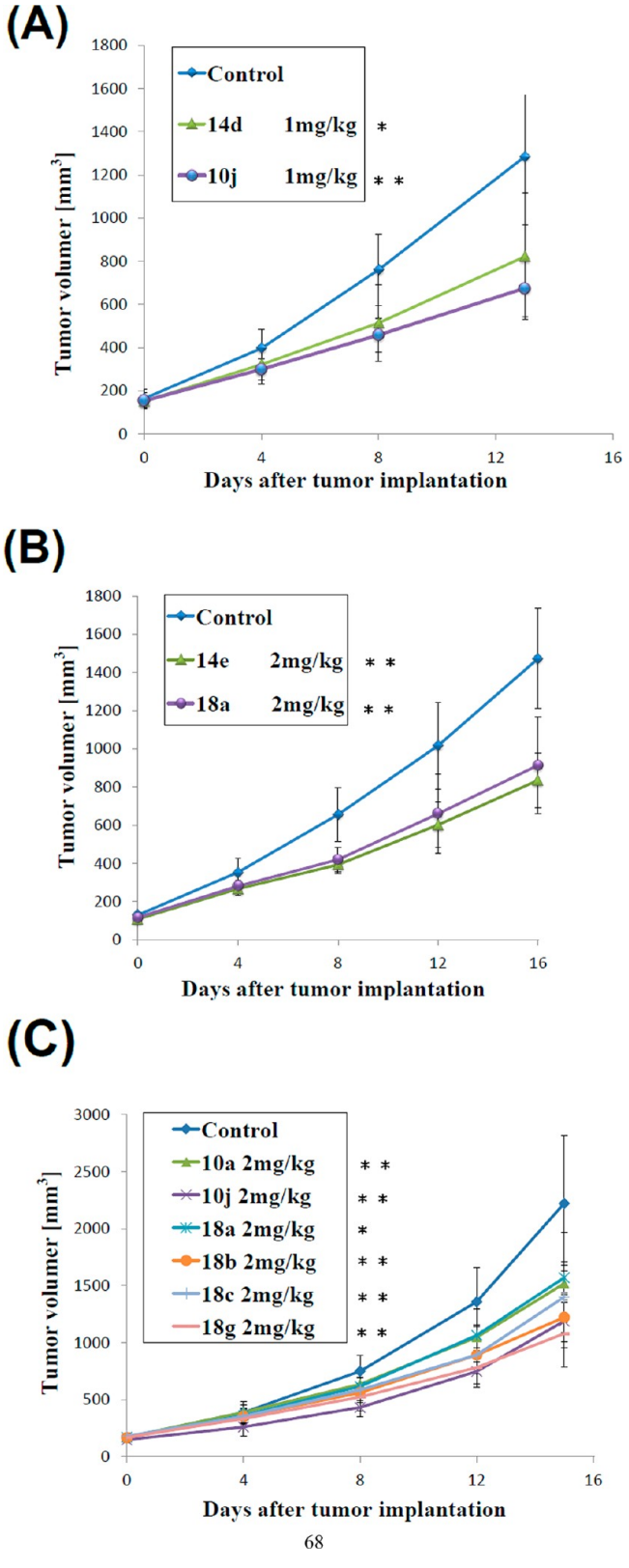

Figure 10. Antitumor efficacy of evodiamine derivatives in the xenograft models. (A) The efficacy of compounds **10j** and **14d** in the A549 xenograft model at the dose of 1 mg/kg. (B) The efficacy of compounds **14e** and **18a** in the A549 xenograft model at the dose of 2 mg/kg. (C) The efficacy of compounds **10a**, **10j**, **18a**, **18b**, **18c**, and **18g** in the HCT116 xenograft model at the dose of 2 mg/kg. Data are presented as the mean ± SEM; $n = 6$ nude mice per group: (*) $P < 0.05$, (**) $P < 0.01$, versus control group, determined with Student's t test.

resistance to Top1 or Top2 inhibitors is an important problem that remains to be solved.[63] It was reported that the emergence of resistance to Top1 inhibitors is often accompanied by a concomitant rise in the level of Top2 expression and vice versa.[67] In this regard, a single compound able to inhibit both Top1 and Top2 could be helpful to prevent mechanism-based drug resistance. Despite the high interest in such compounds, there are relatively few classes of dual inhibitors.[68] The present study discovered evodiamine derivatives as a novel type of dual Top1/Top2 inhibitors. Interestingly, they showed excellent in vitro and in vivo antiproliferative activity with low toxicity. The results preliminary validated the advantages of dual Top1/Top2 inhibitors and the designed compounds represent high-quality antitumor leads for further optimization.

CONCLUSION

Compound **2** represents an attractive lead structure for the development of novel antitumor agents. Inspired by our previous findings, the SAR of compound **2** was investigated systemically. The results highlighted the importance of hydroxyl group on the A-ring and E-ring. Further molecular modeling and mechanism studies confirmed that the derivatives acted by dual inhibition of Top1 and Top2. The hydroxyl group on the scaffold was important for the antitumor activity because it could form important hydrogen bonding interactions with both Top1 and Top2. Furthermore, the introduction of the hydroxyl group is also helpful to improve the water solubility. As a result, a series of highly potent antitumor molecules were identified which showed promising features as antitumor candidates. They showed excellent antiproliferative activity, with their GI_{50} values lower than 3 nM. Moreover, they can effectively induce the apoptosis of cancer cells in A549 cells. Importantly, compounds **10j**, **18b**, **18c**, and **18g** showed good in vivo antitumor efficacy and low toxicity at the dose of 2 mg/kg. They are worthy of further evaluation as potential chemotherapeutic agents. On the other hand, besides Top1 and Top2, there also might be additional targets for the synthesized compounds, which remained to be further identified. Further SAR and target identification studies are in progress.

EXPERIMENTAL SECTION

Chemistry. *General Methods.* ^{1}H NMR and ^{13}C NMR spectra were recorded on Bruker AVANCE300, AVANCE500, or AVANCE600 spectrometer (Bruker Company, Germany), using TMS as an internal standard and $CDCl_3$ or DMSO-d_6 as solvents. Chemical shift are given in ppm (δ). Elemental analyses were performed with a MOD-1106 instrument and were consistent with theoretical values within 0.4%. The mass spectra were recorded on an Esquire 3000 LC-MS mass spectrometer. Silica gel thin-layer chromatography was performed on precoated plates GF-254 (Qingdao Haiyang Chemical, China). Purity of the compounds was analyzed by HPLC (Agilent Technologies 1260 Infinity) using 40:60 MeOH/H_2O as the mobile phase with a flow rate of 0.8 mL/min on a C18 column (Aglilent 20RBA × SB-C18, 5 μm, 4.6 mm × 150 mm). All compounds exhibited greater than 95% purity. All solvents and reagents were analytically pure, and no further purification was needed. All starting materials were commercially available.

*12-Chloroevodiamine (**10a**).* A solution of 8-chloro-4,9-dihydro-3*H*-pyrido[3,4-*b*] indole[69] (**6a**, 0.30 g, 1.5 mmol) and *N*-methyl isatoic anhydride[70] (**9**, 0.26 g, 1.5 mmol) in CH_2Cl_2 (5 mL) was stirred overnight at room temperature. Then target compound **10a** was precipitated from this solution and washed by CH_2Cl_2 to give a white solid (0.29 g, yield 58.2%). ^{1}H NMR ($CDCl_3$, 500 MHz) δ: 2.52 (s, 3H, N_{14}-CH_3), 2.96−2.97 (m, 2H, C_8-H_2), 3.27−3.29 (m, 1H, C_7-H), 4.87−4.90 (m, 1H, C_7-H), 5.94 (s, 1H, C_{13b}-H), 7.12 (t, J = 7.8 Hz, 1H, C_{10}-H), 7.18 (d, J = 8.0 Hz, 1H, C_9-H), 7.24−7.27 (m, 2H), 7.49−7.51 (m, 2H), 8.12 (d, J = 7.8 Hz, 1H, C_4-H), 8.47 (s, 1H, N_{13}-H). ^{13}C NMR

dx.doi.org/10.1021/jm300605m | J. Med. Chem. 2012, 55, 7593−7613

(MeOD, 75 MHz) δ: 19.8, 29.2, 39.4, 68.5, 113.6, 117.0, 118.4, 120.0, 121.1, 121.7, 122.2, 122.7, 126.4, 127.7, 129.1, 133.2, 134.2, 150.9, 165.4. MS (ESI, positive) m/z calcd for $C_{19}H_{17}ClN_3O$ (M + H): 338.81; found 338.61. Anal. ($C_{19}H_{16}ClN_3O$) C, H, N. HPLC purity: 98.3%. The synthetic method for target compounds **10b**−**10g** was similar to that of compound **10a**.

*10-Nitroevodiamine (**10h**).* A solution of KNO_3 (0.67 g, 6.6 mmol) and compound **2** (2 g, 6.6 mmol) in concentrated sulfuric acid (20 mL) was stirred at 0 °C for 12 h. Then the solution was poured to ice−water mixture (100 mL), and a yellow solid was precipitated from the solution. The crude product was collected and purified by silica gel column chromatography (hexane/EtOAc = 3:1) to give **10h** as yellow solid (2.10 g, yield 91.3%). ^{1}H NMR (DMSO-d_6, 500 MHz) δ: 2.89 (s, 3H, N_{14}-CH_3), 2. 94−2.98 (m, 2H, C_8-2H), 3.21−3.26 (m, 1H, C_7-H), 4.63−4.67 (m, 1H, C_7-H), 6.20 (s, 1H, C_{13b}-H), 6.99 (t, J = 7.5 Hz, 1H, C_3-H), 7.07 (d, J = 7.9 Hz, 1H, C_1-H), 7.48−7.53 (m, 2H), 7.80 (d, J = 7.5 Hz, 1H, C_4-H), 8.02 (dd, J = 9.0 Hz, 2.2 Hz, 1H, C_{11}-H), 8.51 (s, 1H, C_9-H), 11.87 (s, 1H, N_{13}-H). ^{13}C NMR (DMSO-d_6, 150 MHz) δ: 19.2, 36.8, 40.7, 69.5, 112.1, 114.2, 115.5, 117.2, 117.6, 119.1, 120.5, 125.3, 128.0, 133.6, 134.9, 139.6, 140.6, 148.5, 164.1. MS (ESI, positive) m/z calcd for $C_{19}H_{17}N_4O_3$ (M + H): 349.36; found 349.91. Anal. ($C_{19}H_{16}N_4O_3$) C, H, N. HPLC purity: 98.1%.

*10,12-Dinitroevodiamine (**10i**).* A solution of KNO_3 (1.33 g, 13.2 mmol) and compound **2** (2 g, 6.6 mmol) in concentrated sulfuric acid (20 mL) was stirred in an ice bath for 12 h. After that, the solution was poured into ice−water mixture (100 mL) and a yellow solid was precipitated from this solution. The crude product was collected and purified by silica gel column chromatography (hexane/EtOAc = 3:1) to give **10i** as yellow solid (1.51 g, yield 58.1%). ^{1}H NMR (DMSO-d_6, 500 MHz) δ: 2.62 (s, 3H, N_{14}-CH_3), 2.90 (m, 2H, C_8-H_2), 3.10−3.18 (m, 1H, C_7-H), 4.65−4.71 (m, 1H, C_7-H), 6.05 (s, 1H, C_{13b}-H), 7.11 (t, J = 7.5 Hz, 1H, C_3-H), 7.22 (d, J = 8.1 Hz, 1H, C_1-H), 7.54 (t, J = 7.8 Hz, 1H, C_2-H), 7.88 (d, J = 7.5 Hz, 1H, C_4-H), 8.83 (s, 1H, C_{11}-H), 9.05 (s, 1H, C_9-H), 12.65 (s, 1H, N_{13}-H). ^{13}C NMR (DMSO-d_6, 150 MHz) δ: 19.7, 35.9, 39.4, 67.7, 114.3, 117.2, 119.5, 121.1, 121.7, 122.0, 128.1, 129.7, 131.2, 131.8, 133.1, 135.7, 139.4, 149.9, 163.6. MS (ESI, negative) m/z calcd for $C_{19}H_{14}N_5O_5$ (M − H): 392.34; found 392.48. Anal. ($C_{19}H_{15}N_5O_5$) C, H, N. HPLC purity: 97.6%.

*10-Hydroxyevodiamine (**10j**).* To a stirred solution of compound **10g** (0.5 g, 1.5 mmol) in CH_2Cl_2 (30 mL), BBr_3 (0.5 mL) was added in one portion and stirred for 6 h at −78 °C. After the addition of methanol (0.4 mL) and CH_2Cl_2 (50 mL), the solution was washed with saturated $NaHCO_3$ aqueous solution (60 mL) and brine (40 mL) and dried over Na_2SO_4, and the solvent was removed under reduced pressure. The residue was purified by silica gel column chromatography (hexane/EtOAc = 2:1) to afford **10j** (0.30 g, yield 63.2%) as white solid. ^{1}H NMR (DMSO-d_6, 500 MHz) δ: 2.65−2.68 (m, 1H, C_8-H), 2.80−2.89 (m, 1H, C_8-H), 2.89 (s, 3H, N_{14}-CH_3), 3.15−3.19 (m, 1H, C_7-H), 4.58−4.62 (m, 1H, C_7-H), 6.08 (s, 1H, C_{13b}-H), 6.61−6.62 (d, 1H, J = 8.5 Hz, C_{11}-H), 6.75 (s, 1H, C_9-H), 6.94 (t, J = 7.5 Hz, 1H, C_3-H), 7.02 (d, J = 8.2 Hz, 1H, C_1-H), 7.14 (d, J = 8.5 Hz, 1H, C_{12}-H), 7.46 (t, J = 7.5 Hz, 1H, C_2-H), 7.78 (d, J = 7.8 Hz, 1H, C_4-H), 8.68 (s, 1H, C_{10}-OH), 10.70 (s, 1H, N_{13}-H). ^{13}C NMR (DMSO-d_6, 75 MHz) δ: 20.0, 31.1, 36.8, 70.4, 102.6, 111.5, 112.5, 112.5, 117.5, 119.5, 120.5, 127.1, 128.4, 131.4, 131.6, 133.9, 149.1, 151.1, 164.7. MS (ESI, positive) m/z calcd for $C_{19}H_{18}N_3O_2$ (M + H): 320.37; found 320.14. Anal. ($C_{19}H_{17}N_3O_2$) C, H, N. HPLC purity: 98.6%. Compound **11e** was synthesized by a similar procedure.

*10-Ethoxyevodiamine (**10k**).* A solution of compound **10j** (0.32 g, 1 mmol), K_2CO_3 (0.16 g, 1.2 mmol), and bromoethane (0.13 g, 1.2 mmol) in ethanol (20 mL) was refluxed for 6 h. Then, the solvent was removed under reduced pressure, and the residue was purified by silica gel column chromatography (hexane/EtOAc = 3:1) to afford **10k** (0.28 g, 79.9%) as a yellow solid. ^{1}H NMR ($CDCl_3$, 500 MHz) δ: 1.45 (t, J = 7.0 Hz, 3H, C_{10}-OCH$_2$C$\underline{H}_3$), 2.51 (s, 3H, N_{14}-CH_3), 2.92 (m, 2H, C_8-H_2), 3.27 (m, 1H, C_7-H), 4.10 (q, J = 7.0 Hz, 2H, C_{10}-OC$\underline{H}_2$CH$_3$), 4.85 (m, 1H, C_7-H), 5.90 (s, 1H, C_{13b}-H), 6.92 (d, J = 8.8 Hz, 1H, C_{11}-H), 7.02 (d, J = 2.0 Hz, 1H, C_9-H), 7.14 (d, J = 7.7 Hz, 1H, C_1-H), 7.23 (t, J = 7.5 Hz,1H, C_3-H), 7.29 (d, J = 8.8 Hz, 1H, C_{12}-H), 7.49 (t, 1H, C_2-H), 8.10−8.12 (m, 2H). ^{13}C NMR ($CDCl_3$, 75 MHz) δ: 15.0, 20.2, 37.2, 39.6, 64.2, 68.9, 101.8, 112.0, 113.4, 113.8, 122.1 (2C), 123.6, 123.9, 126.7, 129.0 (2C), 131.8, 133.1, 153.7, 164.7. MS (ESI, positive) m/z calcd for $C_{21}H_{22}N_3O_2$ (M + H): 348.42; found 348.53. Anal. ($C_{21}H_{21}N_3O_2$) C, H, N. HPLC purity: 99.2%. Compounds **10l**−**10o** were synthesized by a similar procedure.

*1-Methylevodiamine (**14a**).* A solution of 3,4-dihydro-β-carboline **12** (0.05 g, 0.3 mmol) and 1,8-dimethyl-1*H*-benzo[*d*][1,3]oxazine-2,4-dione (0.06 g, 0.3 mmol) in CH_2Cl_2 (10 mL) was stirred at 45 °C for 6 h and then cooled to room temperature. The solvent was concentrated in vacuo, and the crude product was purified by column chromatography (hexane/EtOAc = 5:1) to give compound **14a** (0.08 g, yield 80%) as a white solid. ^{1}H NMR (DMSO-d_6, 500 MHz) δ: 2.18 (s, 3H), 2.42 (s, 3H), 2.82 (m, 1H), 2.93 (m, 1H), 3.19 (m, 1H), 4.25 (m, 1H), 5.94 (s, 1H), 7.04−7.80 (m, 7H), 11.21 (s, 1H). ^{13}C NMR (DMSO-d_6, 150 MHz) δ: 14.3, 16.9, 20.2, 39.3, 69.3, 112.1, 112.1, 118.8, 119.2, 122.4, 124.9, 126.2, 126.3, 127.9, 128.6, 132.7, 134.8, 137.4, 149.5, 164.1. MS (ESI, negative) m/z calcd for $C_{20}H_{18}N_3O$ (M − H): 316.38; found 316.97. Anal. ($C_{20}H_{19}N_3O$) C, H, N. HPLC purity: 98.7%. Compounds **14b**−**14i** and **14m**−**14o** were synthesized by a similar procedure.

*3-Hydroxyevodiamine (**14p**).* To a stirred solution of **14i** (0.1 g, 0.3 mmol) in CH_2Cl_2 (10 mL), a solution of BBr_3 (0.06 mL, 0.6 mmol) in CH_2Cl_2 (5 mL) was added over a period of 2−3 min at −20 °C. The reaction mixture was stirred under nitrogen atmosphere for 5 h, and then 5 mL of methanol was added. The reaction mixture was treated with saturated sodium bicarbonate (50 mL) and extracted with CH_2Cl_2 (3 × 50 mL). The combined organic layers were dried over $MgSO_4$ and filtered. The solvent was removed under reduced pressure, and the residue was purified by silica gel column chromatography (CH_2Cl_2/MeOH = 100:1) to give compound **14p** as a white solid (0.05 g, yield 50%). ^{1}H NMR (DMSO-d_6, 300 MHz) δ: 2.36 (s, 3H), 2.79−2.82 (m, 2H), 3.13−3.16 (m, 1H), 4.62−4.66 (m, 1H), 5.95 (s, 1H), 6.93−7.13 (m, 5H), 7.28 (d, J = 2.7 Hz, 1H), 7.36 (d, J = 8.1 Hz, 1H), 7.50 (d, J = 8.1 Hz, 1H), 9.45 (s, 1H), 11.25 (s, 1H). ^{13}C NMR (DMSO-d_6, 150 MHz) δ: 19.8, 36.9, 39.3, 68.9, 111.5, 111.59, 113.1, 118.3, 118.8, 120.8, 121.8, 123.5, 123.8, 125.7, 129.3, 136.8, 142.6, 153.4, 163.6. MS (ESI, negative) m/z calcd for $C_{19}H_{16}N_3O_2$ (M − H): 318.35; found 318.82. Anal. ($C_{19}H_{17}N_3O_2$) C, H, N. HPLC purity: 98.3%. The synthetic method for compound **14q** was similar to the synthesis of compound **14p**.

*4-Hydroxyevodiamine (**14q**).* White solid (0.054 g, yield 52%). ^{1}H NMR (DMSO-d_6, 300 MHz) δ: 2.79−2.80 (m, 1H), 2.93−2.95 (m, 1H), 2.99 (s, 3H), 3.20−3.23 (m, 1H), 4.57−4.60 (m, 1H), 6.24 (s, 1H), 6.28 (d, J = 8.4 Hz, 1H), 6.38 (d, J = 8.4 Hz, 1H), 6.99 (t, J = 7.5 Hz, 1H), 7.10 (t, J = 7.5 Hz, 1H), 7.27−7.36 (m, 2H), 7.45 (d, J = 7.5 Hz, 1H), 11.00 (s, 1H), 12.51 (s, 1H). ^{13}C NMR (acetone-d_6, 150 MHz) δ: 21.0, 38.1, 42.0, 71.9, 105.3, 108.9, 110.4, 113.0 113.6, 119.8, 120.7, 123.7, 127.9, 131.6, 136.6, 138.4, 151.2, 163.7, 170.9. MS (ESI, negative) m/z calcd for $C_{19}H_{16}N_3O_2$ (M − H): 318.35; found 318.94. Anal. ($C_{19}H_{17}N_3O_2$) C, H, N. HPLC purity: 97.6%.

*3-Aminoevodiamine (**14r**).* 10% Pd/C (0.01 g) was added to a stirring solution of **14j** (0.12 g, 0.34 mmol) in DMF (10 mL), and the reaction mixture was stirred under hydrogen atmosphere for 12 h at room temperature. The mixture was diluted with water (50 mL) and then extracted with EtOAc (3 × 50 mL). The combined organic layers were washed with saturated sodium chloride solution (3 × 50 mL), dried over anhydrous Na_2SO_4, and concentrated under reduced pressure. The residue was purified by silica gel column chromatography (gradient CH_2Cl_2/MeOH = 100:1 to 100:2) to give compound **14r** as a yellow solid (0.08 g, yield 73%). ^{1}H NMR (DMSO, 500 MHz) δ: 2.27 (s, 3H), 2.77−2.79 (m, 1H), 2.88−2.92 (m, 1H), 3.11−3.13 (m, 1H), 4.63−4.67 (m, 1H), 5.10 (s, 2H), 5.90 (s, 1H), 6.78 (dd, J = 8.5 Hz, 2.5 Hz, 1H), 6.94 (d, J = 8.5 Hz, 1H), 7.01 (t, J = 7.5 Hz, 1H), 7.10−7.14 (m, 2H), 7.36 (d, J = 8.0 Hz, 1H), 7.51 (d, J = 8.0 Hz, 1H), 11.26 (s, 1H). ^{13}C NMR (DMSO-d_6, 75 MHz): δ 20.11, 36.98, 39.23, 69.53, 111.75, 112.05, 112.54, 118.55, 119.18, 120.27, 122.21, 123.91, 124.34, 126.21, 129.42, 137.28, 141.46, 145.26, 164.87. MS (ESI, positive) m/z calcd for $C_{19}H_{19}N_4O$ (M + H): 319.38; found 319.93. Anal. ($C_{19}H_{18}N_4O$) C, H, N. HPLC purity: 98.9%. The synthetic method for target compounds **18f** was similar to the synthesis of compound **14r**.

*3-(Azetidin-1-yl)evodiamine (**15a**).* To a stirred mixture of compound **14r** (0.1 g, 0.31 mmol), potassium carbonate (0.08 g, 0.62 mmol),

dx.doi.org/10.1021/jm300605m | J. Med. Chem. 2012, 55, 7593−7613

and DMSO (5 mL), 1,3-dibromopropane (0.25 g, 1.24 mmol) was added dropwise within 1 h at room temperature. Then the mixture was heated to 60 °C and stirred for 7 h. After cooling, the mixture was diluted with water (50 mL) and extracted with EtOAc (3 × 50 mL). The organic layer was dried over Na_2SO_4, and the solvent was evaporated in vacuo. The crude product was purified by silica gel column chromatography (CH_2Cl_2/MeOH = 100:2) to give compound **15a** as a red solid. (0.03 g, yield 27%). ^{1}H NMR (DMSO-d_6, 300 MHz) δ: 2.28 (t, J = 7.2 Hz, 2H), 2.35 (s, 3H), 2.80−2.83 (m, 2H), 3.10−3.13 (m, 1H), 3.79 (t, J = 7.2 Hz, 4H), 4.62−4.67 (m, 1H), 5.94 (s, 1H), 6.64 (dd, J = 8.4 Hz, 2.7 Hz, 1H), 6.88 (d, J = 2.7 Hz, 1H), 6.98−7.12 (m, 3H), 7.35 (d, J = 7.8 Hz, 1H), 7.49 (d, J = 7.8 Hz, 1H), 11.26 (s, 1H). ^{13}C NMR (DMSO-d_6, 150 MHz) δ: 13.5, 16.5, 18.7, 19.8, 37.1, 52.1, 69.0, 109.1, 111.5, 111.6, 116.8, 118.3, 118.8, 121.8, 123.1, 123.4, 125.7, 129.4, 136.8, 141.2, 148.7, 163.8. MS (ESI, positive) m/z calcd for $C_{22}H_{23}N_4O$ (M + H): 359.44; found 359.76. Anal. ($C_{22}H_{22}N_4O$) C, H, N. HPLC purity: 98.4%.

*3-Acetamidoevodiamine (**15c**).* Compound **14r** (0.1 g, 0.3 mmol) and triethylamine (0.04 mL, 0.3 mmol) were dissolved in CH_2Cl_2 (15 mL). Acetic anhydride (0.05 g, 0.47 mmol) was added dropwise within 30 min, and the mixture was stirred at room temperature for 2 h. The precipitate was collected by filtration and washed with alcohol to give **15c** (0.09 g, yield 82%) as a red solid. ^{1}H NMR (DMSO-d_6, 300 MHz) δ: 2.04 (s, 3H), 2.67 (s, 3H), 2.83−2.85 (m, 2H), 3.19−3.23 (m, 1H), 4.59−4.63 (m, 1H), 5.93 (s, 1H), 7.00 (t, J = 7.8 Hz, 1H), 7.08−7.13 (m, 2H), 7.35 (d, J = 7.8 Hz, 1H), 7.48 (d, J = 7.8 Hz, 1H), 7.73 (dd, J = 9.0 Hz, 2.7 Hz, 1H), 8.04 (d, J = 2.7 Hz, 1H), 10.23 (s, 1H), 11.27 (s, 1H). ^{13}C NMR (DMSO-d_6, 75 MHz) δ: 19.6, 23.8, 36.5, 55.0, 69.2, 111.6, 111.6, 118.2, 118.3, 118.8, 120.1, 121.2, 121.9, 124.5, 125.8, 129.8, 133.8, 136.7, 145.1, 163.8, 168.0. MS (ESI, positive) m/z calcd for $C_{21}H_{21}N_4O_2$ (M + H): 361.42; found 361.96. Anal. ($C_{21}H_{20}N_4O_2$) C, H, N. HPLC purity: 97.6%.

*3-Fluoro-10-methoxyevodiamine (**17a**).* Reaction of 6-methoxy-3,4-dihydro-β-carboline **6g** (0.3 g, 1.5 mmol) and 1-methyl-6-fluoro-1*H*-benzo[*d*][1,3]oxazine-2,4-dione (0.2 g, 1.0 mmol) as described for the synthesis of **14a**, followed by purification using silica gel column chromatography (hexane/EtOAc = 3:1) gave **17a** (0.25 g, yield 71%) as a white solid. ^{1}H NMR (DMSO-d_6, 300 MHz) δ: 2.86 (s, 3H), 3.03−3.06 (m, 2H), 3.38−3.40 (m, 1H), 3.95 (s, 3H), 4.79−4.83 (m, 1H), 6.26 (s, 1H), 6.95 (dd, J = 8.7 Hz, 2.4 Hz, 1H), 7.19 (d, J = 2.4 Hz, 1H), 7.35−7.39 (m, 1H), 7.44 (d, J = 9.0 Hz, 1H), 7.54−7.61 (m, 1H), 7.72 (d, J = 9.0 Hz, 3.3 Hz, 1H), 11.21 (s, 1H). ^{13}C NMR (DMSO-d_6, 75 MHz) δ: 19.6, 36.6, 55.3, 69.3, 100.1, 111.4, 112.1, 112.3, 113.2, 113.5, 120.4, 121.6, 122.0, 126.1, 130.2, 131.7, 146.0, 153.4, 163.0. MS (ESI, positive) m/z calcd for $C_{20}H_{19}FN_3O_2$ (M + H): 352.38; found 352.92. Anal. ($C_{20}H_{18}FN_3O_2$) C, H, N. HPLC purity: 99.2%. The synthetic method for target compounds **17b−17e** was similar to the synthesis of compound **17a**.

*3-Fluoro-10-hydroxyevodiamine (**18a**).* Reaction of **17a** (0.1 g, 0.28 mmol) and BBr_3 (0.06 mL, 0.6 mmol) as described for the synthesis of **14p**, followed by purification using silica gel column chromatography (CH_2Cl_2/MeOH = 100:1) gave **18a** as a white solid (0.05 g, yield 52%). ^{1}H NMR (DMSO-d_6, 600 MHz) δ: 2.67 (s, 3H), 2.72−2.73 (m, 1H), 2.75−2.81 (m, 1H), 3.14−3.18 (m, 1H), 4.56−4.59 (m, 1H), 6.02 (s, 1H), 6.29 (dd, J = 9.0 Hz, 2.4 Hz, 1H), 6.76 (d, J = 2.4 Hz, 1H), 7.13−7.15 (m, 2H), 7.33−7.36 (m, 1H), 7.51 (dd, J = 9.0 Hz, 2.4 Hz, 1H), 8.67 (s, 1H), 10.79 (s, 1H). ^{13}C NMR (DMSO-d_6, 150 MHz) δ: 20.0, 37.0, 40.9, 69.8, 102.7, 111.2, 112.5, 112.7, 113.7, 113.9, 120.9, 121.0, 121.8, 127.0, 130.5, 131.5, 146.4, 151.2, 163.5. ESI-MS MS (ESI, negative) m/z calcd for $C_{19}H_{15}FN_3O_2$ (M − H): 336.34; found 336.84. Anal. ($C_{19}H_{16}FN_3O_2$) C, H, N. HPLC purity: 98.7%. Compounds **18b−18e** and **18g** were synthesized by a similar procedure.

*3-Amino-10-hydroxyevodiamine (**18g**).* Yellow solid (0.03 g, yield 31%). ^{1}H NMR (DMSO-d_6, 600 MHz) δ: 2.27 (s, 3H), 2.49−2.51 (m, 2H), 2.68−2.70 (m, 1H), 5.09 (s, 2H), 5.84 (s, 1H), 6.62 (dd, J = 8.4 Hz, 2.4 Hz, 1H), 6.76 (dd, J = 8.4 Hz, 2.4 Hz, 1H), 6.79 (d, J = 2.4 Hz, 1H), 6.93 (d, J = 2.4 Hz, 1H), 7.12−7.15 (m, 2H), 8.67 (s, 1H), 10.90 (s, 1H). ^{13}C NMR (DMSO-d_6, 75 MHz) δ: 19.9, 37.0, 48.6, 69.0, 102.3, 110.6, 111.7, 111.9, 112.0, 119.4, 123.4, 123.9, 126.4, 129.8, 131.3, 140.3, 145.1, 150.6, 164.0. MS (ESI, positive) m/z calcd for $C_{19}H_{19}N_4O_2$ (M + H): 335.38; found 335.85. Anal. ($C_{19}H_{18}N_4O_2$) C, H, N. HPLC purity: 98.5%.

*5-Thioxoevodiamine (**19**).* To a stirred solution of compound **2** (0.3 g, 1 mmol) in toluene (30 mL), Lawesson's reagent (0.61 g, 1.5 mmol) was added and stirred for 6 h at 110 °C. Then the solvent was removed under reduced pressure. The residue was purified by silica gel column chromatography (hexane/EtOAc = 4:1) to afford **19** as a yellow solid (0.21 g, yield 65.6%). ^{1}H NMR ($CDCl_3$, 500 MHz) δ: 2.45 (s, 3H), 3.03−3.09 (m, 2H), 3.81−3.90 (m, 1H), 5.56−5.62 (m, 1H), 5.75 (s, 1H), 7.10 (d, J = 8.1 Hz, 1H), 7.16−7.23 (m, 2H), 7.29 (d, J = 7.5 Hz, 1H), 7.42−7.49 (m, 2H), 7.63 (d, J = 7.8 Hz, 1H), 8.30 (s, 1H), 8.56 (d, J = 8.1 Hz, 1H). ^{13}C NMR ($CDCl_3$, 75 MHz) δ: 19.6, 35.3, 47.5, 69.7, 111.3, 112.5, 115.4, 118.3, 119.4, 120.0, 121.7, 122.5, 126.4, 127.8, 132.4, 132.8, 136.6, 145.5, 190.7. MS (ESI, positive) m/z calcd for $C_{19}H_{18}N_3S$ (M + H): 320.43; found 320.90. Anal. ($C_{19}H_{17}N_3S$) C, H, N. HPLC purity: 99.5%. Compounds **23** was synthesized by a similar procedure.

*5-(Methylene)evodiamine (**21**).* To a stirred solution of compound 2 (0.3 g, 1 mmol) in THF (30 mL), $LiAlH_4$ (0.11 g, 3 mmol) was added and the mixture was stirred for 12 h at room temperature. After the addition of H_2O (0.2 mL), the solvent was removed under reduced pressure. The residue was purified by silica gel column chromatography (hexane/EtOAc = 4:1) to afford **21** as a pale solid (0.17 g, yield 58.6%). ^{1}H NMR (500 MHz, $CDCl_3$) δ: 2.66 (s, 3H), 2.81(m, 2H), 3.05 (m, 1H), 3.34 (m, 1H), 3.86 (d, J = 13.1 Hz, 1H), 4.07 (d, J = 14.1 Hz, 1H), 4.82 (s, 1H), 6.95 (d, J = 7.2 Hz, 1H), 6.99−7.07 (m, 2H), 7.10−7.23 (m, 3H), 7.36 (d, J = 7.8 Hz, 1H), 7.55 (d, J = 7.5 Hz, 1H), 8.24 (s, 1H). ^{13}C NMR ($CDCl_3$, 75 MHz) δ: 20.6, 39.1, 50.1, 55.7, 73.6, 110.7 (2C), 111.4, 118.1 (2C), 119.1 (2C), 121.5, 121.8, 126.4, 126.7, 130.4, 136.0, 148.0. MS (ESI, positive) m/z calcd for $C_{19}H_{20}N_3$ (M + H): 290.38; found 290.53. Anal. ($C_{19}H_{19}N_3$) C, H, N. HPLC purity: 99.1%.

*3-Fluoro-10-methoxy-7,8,13b,14-tetrahydroindolo[2′,3′:3,4]-pyrido[2,1-b]quinazolin-5(13H)-one (**25a**).* A solution of intermediate **6g** (1 g, 5.0 mmol) and **24** (0.90 g, 5.0 mmol) in CH_2Cl_2 (30 mL) was stirred for 6 h at room temperature. Then, the target compound **25a** was precipitated from the solvent as a pale solid (1.42 g, yield 84.1%). ^{1}H NMR ($CDCl_3$, 600 MHz) δ: 2.90−2.92 (m, 2H), 3.15−3.20 (m, 1H), 3.87 (s, 3H), 4.98−5.02 (m, 1H), 5.87 (s, 1H), 6.91 (dd, J = 9.0 Hz, 2.4 Hz, 1H), 6.98 (dd, J = 8.4 Hz, 4.2 Hz, 1H), 7.00 (d, J = 2.4 Hz, 1H), 7.14 (t, J = 8.4 Hz, 1H), 7.28 (d, J = 8.4 Hz, 1H), 7.79 (dd, J = 8.4 Hz, 3.0 Hz, 1H), 8.11 (s, 1H). ^{13}C NMR (DMSO-d_6, 150 MHz) δ: 20.0, 38.7, 55.3, 63.8, 100.3, 109.2, 111.9, 112.3, 113.3, 117.2, 120.7, 126.1, 131.0, 131.3, 143.7, 153.4, 154.8, 156.3, 162.7. MS (ESI, positive) m/z calcd for $C_{19}H_{17}FN_3O_2$ (M + H): 338.36; found 338.21. Anal. ($C_{19}H_{16}FN_3O_2$) C, H, N. HPLC purity: 98.8%. Compound **25b** was synthesized by a similar procedure.

*3-Fluoro-10-methoxyrutecarpine (**26a**).* To a solution of compound **25a** (0.50 g, 1.5 mmol) in DMSO (20 mL), IBX (0.41 g, 1.5 mmol) was added and stirred for 2 h at room temperature. Then H_2O (40 mL) was added and extracted with EtOAc (3 × 30 mL). The combined organic phases were dried over Na_2SO_4, and the solvent was removed under reduced pressure. The residue was purified by silica gel column chromatography (hexane/EtOAc = 3:1) to afford **26a** as a pale solid (0.44 g, yield 86.7%). ^{1}H NMR ($CDCl_3$, 600 MHz) δ: 3.22 (t, J = 7.2 Hz, 2H), 3.88 (s, 3H), 4.57 (t, J = 7.2 Hz, 2H), 7.01 (s, 1H), 7.03 (d, J = 9.6 Hz, 1H), 7.36 (d, J = 8.4 Hz, 1H), 7.45 (t, J = 9.6 Hz, 1H), 7.70 (s, 1H), 7.94 (dd, J = 8.4 Hz, 3.0 Hz, 1H), 9.02 (s, 1H). ^{13}C NMR (DMSO-d_6, 75 MHz) δ: 19.4, 31.1, 55.8, 100.9, 111.6, 113.9, 116.4, 117.9, 122.1, 123.2, 125.5, 127.7, 129.6, 134.4, 144.8, 145.3, 154.3, 159.2, 160.5. MS (ESI, positive) m/z calcd for $C_{19}H_{15}FN_3O_2$ (M + H): 336.34; found 336.96. HPLC purity: 98.2%. The synthetic method for compound **26b** was similar to the synthesis of compound **26a**.

*7,8,13,13b-Tetrahydro-5H-benzo[5′,6′][1,3]oxazino[3′,2′:1,2]-pyrido[3,4-b]indol-5-one (**28**).* To a solution of 2-hydroxybenzoic acid (1 g, 7.2 mmol) in CH_2Cl_2 (50 mL), sulfurous dichloride (1.71 g, 14.4 mmol) was added and stirred for 1 h at 40 °C. Then the solvent and excess sulfurous dichloride were removed under reduced pressure. The residue was added to a solution of intermediate **12** (1.02 g, 6 mmol) in CH_2Cl_2 (30 mL) and stirred for 12 h at room temperature After reaction, the solvent was removed under reduced pressure and the residue was purified by silica gel column chromatography (hexane/EtOAc = 4:1) to

dx.doi.org/10.1021/jm300605m | J. Med. Chem. 2012, 55, 7593−7613

afford **28** as a white solid (1.01 g, yield 57.6%). ^{1}H NMR (DMSO-d_6, 500 MHz) δ: 2.93−3.02 (m, 2H), 3.21−3.22 (m, 1H), 4.71−4.74 (m, 1H), 6.68 (s, 1H), 7.07 (t, J = 7.7 Hz, 1H), 7.13−7.27 (m, 3H), 7.42 (d, J = 8.2 Hz, 1H), 7.57−7.60 (m, 2H), 7.91 (d, J = 7.6 Hz, 1H), 11.52 (s, 1H). ^{13}C NMR ($CDCl_3$, 75 MHz) δ: 14.1, 39.1, 81.2, 111.6, 113.7, 116.3, 118.6, 119.3, 120.3, 123.0, 123.7, 125.9, 127.1, 128.8, 134.2, 137.2, 156.7, 163.0. MS (ESI, positive) m/z calcd for $C_{18}H_{15}N_2O_2$ (M + H): 291.32; found 291.43. Anal. ($C_{18}H_{14}N_2O_2$) C, H, N. HPLC purity: 98.6%.

*6-Benzyloxy-2,3,4,9-tetrahydro-1H-β-carbolin-1-one (**35**).* 4-(Benzyloxy)aniline (1.4 g, 5.8 mmol) was dissolved in 3 M hydrochloric acid (10 mL). A solution of sodium nitrite (0.5 g, 8.7 mmol) in water (5 mL) was added dropwise within 30 min. After stirring for 2 h under the temperature lower than 5 °C, the solution of ethyl 2-oxopiperidine-3-carboxylate (1.0 g, 5.8 mmol) and KOH (0.4 g, 6.9 mmol) in water (20 mL), which had been stirred for 12 h at room temperature, was added under the ice−water bath condition. Then the reaction mixture was further stirred for 10 h at room temperature. The brown precipitate was filtered and washed with water to give the crude product **34**, which was dissolved in 98% HCOOH (15 mL). The mixture was heated to 110 °C for 0.5 h and then cooled to room temperature. Next, the reaction was poured into cold water to afford a red mixture that was extracted three times with EtOAc. The organic layer was dried over Na_2SO_4, and the solvent was removed under reduced pressure. The residue was purified by flash chromatography (CH_2Cl_2/MeOH = 100:2) to give the title compound **35** as a brown solid (1.1 g, yield 59%). ^{1}H NMR (DMSO-d_6, 300 MHz) δ: 2.86 (t, J = 6.6 Hz, 2H), 3.47 (t, J = 6.6 Hz, 2H), 5.09 (s, 2H), 6.93 (m, 1H), 7.16 (d, J = 1.8 Hz, 1H), 7.25−7.47 (m, 6H), 7.53 (s, 1H), 11.45 (s, 1H). MS (ESI, positive) m/z calcd for $C_{18}H_{17}N_2O_2$ (M + H): 293.33; found 293.38. Anal. ($C_{18}H_{16}N_2O_2$) C, H, N. HPLC purity: 99.1%.

*3-Fluoro-10-benzyloxydehydroevodiamine (**37**).* To a stirring solution of **35** (0.3 g, 1 mmol) in dry THF (20 mL) was added $POCl_3$ (0.14 mL, 1.5 mmol) at 60 °C, and the mixture was stirred under nitrogen atmosphere at the same temperature. After 40 min, methyl 5-fluoro-2-(methylamino)benzoate (0.28 g, 1.5 mmol) was added and the reaction mixture was stirred under reflux for 3 days. The mixture was diluted with water (100 mL) and then extracted with EtOAc (3 × 100 mL). The combined organic layers were washed with saturated sodium chloride solution (3 × 100 mL), dried over anhydrous Na_2SO_4, and concentrated under reduced pressure. The residue was purified by column chromatography (gradient CH_2Cl_2/MeOH = 100:2 to 100:5) to give compound **37** as a yellow solid (0.23 g, yield 50%). ^{1}H NMR (DMSO-d_6, 600 MHz) δ: 3.13 (t, J = 7.2 Hz, 2H), 4.01 (s, 3H), 4.45 (t, J = 7.2 Hz, 2H), 5.11 (s, 2H), 7.03 (dd, J = 9.0 Hz, 2.5 Hz, 1H), 7.06 (dd, J = 9.4 Hz, 3.0 Hz, 1H), 7.14−7.18 (m, 1H), 7.24 (d, J = 2.4 Hz, 1H), 7.29−7.32 (m, 2H), 7.36−7.39 (m, 3H), 7.44 (d, J = 7.8 Hz, 1H), 7.47 (d, J = 1.4 Hz, 1H), 11.60 (s, 1H).

*(S)-3-Fluoro-10-benzyloxyevodiamine (S-**38**).* To a stirred solution of **37** (50 mg, 0.11 mmol) and RuCl[(*S*,*S*)-Tsdpen](*p*-cymene) (4 mg, 6 mmol %) in DMF (2.5 mL) was added a 5:2 HCO_2H−triethylamine (18 μL). Then the reaction mixture was stirred at 0 °C for 8 h, diluted with water (15 mL), and extracted with EtOAc (3 × 15 mL). The organic layer was dried over Na_2SO_4, and the solvent was evaporated in vacuo. The residue was purified by column chromatography (hexane/EtOAc = 4:1) to give compound (*S*)-**38** as a white solid (40 mg, yield 87%). ^{1}H NMR (DMSO-d_6, 600 MHz) δ: 2.65 (s, 3H), 2.77−2.83 (m, 1H), 3.14−3.19 (m, 1H), 4.58−4.61 (m, 1H), 5.07 (s, 2H), 6.04 (s, 1H), 6.83 (dd, J = 8.7 Hz, 2.4 Hz, 1H), 7.08 (d, J = 2.4 Hz, 1H), 7.16 (dd, J = 8.9 Hz, 4.5 Hz, 1H), 7.24 (d, J = 8.7 Hz, 1H), 7.29 (t, J = 7.3 Hz, 1H), 7.33−7.38 (m, 3H), 7.45 (d, J = 7.6 Hz, 2H), 7.52 (dd, J = 8.8 Hz, 3.1 Hz, 1H), 10.99 (s, 1H). MS (ESI, positive) m/z calcd for $C_{26}H_{23}FN_3O_2$ (M + H): 428.48; found 428.35. Anal. ($C_{26}H_{22}FN_3O_2$) C, H, N. HPLC (Daicel Chiralpak AS, i-PrOH/hexane = 30/70, flow rate = 0.8 mL/min, λ = 254 nm): t_{major} = 15.87 min, t_{minor} = 37.87 min, *ee* = 99%. $[\alpha]_D^{22}$ = +333° (c = 3.0 mg/mL, acetone).

*(R)-3-Fluoro-10-benzyloxyevodiamine (R-**38**).* The synthetic method for compound (*R*)-**38** was similar to that of compound (*S*)-**38**. White solid, yield 83%. HPLC (Daicel Chiralpak AS, i-PrOH/hexane = 30/70, flow rate = 0.8 mL/min, λ = 254 nm): t_{major} = 37.87 min, t_{minor} = 15.87 min, *ee* = 99%. $[\alpha]_D^{22}$ = −351° (c = 1.3 mg/mL, acetone).

*(S)-3-Fluoro-10-hydroxyevodiamine (S-**18a**).* A solution of (*S*)-**38** (30 mg, 0.07 mmol) and 10% Pd/C (3 mg) in EtOAc (10 mL) was stirred under hydrogen atmosphere at room temperature for 12 h. The mixture was filtered, and the solvent was evaporated under reduced pressure. The residue was purified by column chromatography (hexane/EtOAc = 3:1) to give compound (*S*)-**18a** as a white solid (20 mg, yield 86%). ^{1}H NMR (DMSO-d_6, 500 MHz) δ: 2.68 (s, 3H), 2.72−2.74 (m, 2H), 2.76−2.83 (m, 1H), 4.58−4.61 (m, 1H), 6.04 (s, 1H), 6.62 (dd, J = 8.6 Hz, 2.1 Hz, 1H), 6.77 (s, 1H), 7.14−7.17 (m, 2H), 7.37 (d, J = 3.0 Hz), 7.52 (dd, J = 8.8 Hz, 2.9 Hz, 1H), 8.69 (s, 1H), 10.81 (s, 1H). MS (ESI, negative) m/z calcd for $C_{19}H_{15}FN_3O_2$ (M − H): 336.34; found 336.84. HPLC (Daicel Chiralpak AD, i-PrOH/hexane = 30/70, flow rate = 0.8 mL/min, λ = 254 nm): t_{major} = 7.09 min, t_{minor} = 10.09 min, *ee* = 90%. $[\alpha]_D^{22}$ = +341° (c = 2.6 mg/mL, acetone).

*(R)-3-Fluoro-10-hydroxyevodiamine (R-**18a**).* The synthetic method for compound (*R*)-**18a** was similar to that of compound (*S*)-**18a**. White solid, yield 85%. HPLC (Daicel Chiralpak AD, i-PrOH/hexane = 30/70, flow rate = 0.8 mL/min, λ = 254 nm): t_{major} = 9.04 min, t_{minor} = 7.14 min, *ee* = 90%. $[\alpha]_D^{22}$ = −374° (c = 2.0 mg/mL, acetone).

Top1 Inhibitory Activity Assay. DNA relaxation assays were employed according to the procedure described in previous studies.[45] The reaction mixture contained 35 mM Tris-HCl (pH 8.0), 72 mM KCl, 5 mM $MgCl_2$, 5 mM dithiothreitol, 5 mM spermidine, 0.1% bovine serum albumin (BSA), pBR322 plasmid DNA (0.25 μg), the indicated drug concentrations (1% DMSO), and 1 unit of Top1 (TaKaRa Biotechnology Co., Ltd., Dalian) in a final volume of 20 μL. Reaction mixtures were incubated for 15 min at 37 °C and stopped by addition of 2 μL of 10× loading buffer (0.9% sodium dodecyl sulfate (SDS), 0.05% bromophenol blue, and 50% glycerol). Electrophoresis was carried out in a 0.8% agarose gel in TAE (Tris-acetate-EDTA) at 8 V/cm for 1 h. Gels were stained with ethidium bromide (0.5 μg/mL) for 60 min. The DNA band was visualized over UV light and photographed with Gel Doc Ez imager (Bio-Rad Laboratories Ltd.).

Top2 Inhibitory Activity Assay. DNA Top2α inhibitory activity of the compounds was measured using Topoisomerase II Drug Screening Kit (TopoGEN, Inc.). The reaction mixture contained 50 mM Tris-HCl (pH 8.0), 150 mM NaCl, 10 mM $MgCl_2$, 5 mM dithiothreitol, 30 μg/mL bovine serum albumin (BSA), 2 mM ATP, pBR322 plasmid DNA (0.25), the indicated drug concentrations (1% DMSO), and 0.75 unit of Top2α (TopoGEN, Inc.) in a final volume of 20 μL. Reaction mixtures were incubated for 30 min at 37 °C and stopped by addition of 2 μL of 10% SDS. After that, 2 μL of 10× gel loading buffer (0.25% bromophenol blue, 50% glycerol) was added. The reaction products were analyzed on 1% agarose gel at 8 V/cm for 1 h with TAE (Tris-acetate-EDTA) as the running buffer. Gels were stained with ethidium bromide (0.5 μg/mL) for 60 min. The DNA band was visualized over UV light and photographed with Gel Doc Ez imager (Bio-Rad Laboratories Ltd.).

Absorbance Titration. Interaction between the investigational compounds and DNA was evaluated by absorbance titration.[71−73] The calf thymus DNA (ct-DNA, purchased from Sigma-Aldrich) was dissolved in DPBS (2.67 mM KCl, 1.47 mM KH_2PO_4, 137.93 mM NaCl, 8.06 mM Na_2HPO_4, pH 7.4). DNA concentration was determined by UV absorbance at 260 nm using the molar absorption coefficient 13200 M^{-1}/cm in units of DNA bp. Various compounds (50 μM) were prepared in DPBS with 1% DMSO in the presence or absence of increasing concentrations of ct-DNA (0−100 μM). Absorption spectra were recorded in the 220−400 nm spectral range after equilibration at room temperature for 20 min using Synergy 2 multimode microplate reader (BioTek Instruments, Inc.).

Top1 Unwinding Assay. Unwinding assays was employed to determine whether test compounds could intercalate into plasmid DNA.[57,61] The compounds (100 μM) or ethidium bromide (1 μg/mL) were incubated with pBR322 plasmid DNA (0.25 μg) at 37 °C for 15 min in 20 μL of Top1 buffer (35 mM Tris-HCl (pH 8.0), 72 mM KCl, 5 mM $MgCl_2$, 5 mM dithiothreitol, 5 mM spermidine, 0.1% BSA) to ensure binding equilibrium. Five units of Top1 (TaKaRa Biotechnology (Dalian) Co., Ltd.) was added to the reaction mixture and incubated at 37 °C for 60 min to ensure relaxation of the DNA. The reaction mixture was stopped by the sequential addition of 2 μL of 10% SDS and 2 μL of

dx.doi.org/10.1021/jm300605m | J. Med. Chem. 2012, 55, 7593−7613

proteinase K at 2 mg/mL for 20 min at 50 °C. After extraction with an equal volume of phenol/chloroform/isoamyl alcohol (25:24:1), the samples were processed as described in the Top1 relaxation assay.

Top2-Mediated DNA Cleavage Assay. The same Top2 drug screening kit was used as above, but this time an amount of 8 units of hTop2α was added.[74,75] Proteinase K (200 μg/mL final concentration) was added, and the samples were incubated at 50 °C for 20 min. Electrophoresis was run in TAE with 0.5 μg/mL ethidium bromide.

Top1-Mediated DNA Cleavage Assay. DNA cleavage assay was performed as previously described.[76,77] In brief, 20 μL volumes containing 35 mM Tris-HCl (pH 8.0), 72 mM KCl, 5 mM $MgCl_2$, 5 mM dithiothreitol, 5 mM spermidine, 0.1% BSA, pUC19 plasmid DNA (0.25 μg), 4 units of Top1 (TaKaRa Biotechnology (Dalian) Co.,Ltd.), and the indicated drug concentrations (1% DMSO) was incubated for 15 min at 37 °C and stopped by the addition of 2 μL of 10% SDS. Proteinase K (200 μg/mL final concentration) was added, and the samples were incubated at 50 °C for 20 min. After that, 2 μL of 10× gel loading buffer (0.25% bromophenol blue, 50% glycerol) was added. The samples were analyzed on 1% agarose (containing 0.5 μg/mL ethidium bromide) at 8 V/cm for 1 h with TAE as the running buffer. The DNA band was visualized over UV light and photographed with Gel Doc Ez imager (Bio-Rad Laboratories, Ltd.).

In Vitro Cytotoxicity Assay. Cells were plated in 96-well microtiter plates at a density of 5×10^3/well and incubated in a humidified atmosphere with 5% CO_2 at 37 °C for 24 h. Test compounds were added onto triplicate wells with different concentrations and 0.1% DMSO for control. After they had been incubated for 72 h, 20 μL of MTT (3-(4,5-dimethylthiazol-2-yl)-2,5-diphenyltetrazolium bromide) solution (5 mg/mL) was added to each well and the plate was incubated for an additional 4 h. The formazan was dissolved in 100 μL of DMSO. The absorbance (OD) was read on a WellscanMK-2 microplate reader (Labsystems) at 570 nm. The concentration causing 50% inhibition of cell growth (GI_{50}) was determined by the Logit method.[61,75] All experiments were performed three times.

Apoptosis Detection Assay. A549 cells (5×10^5 cells/mL) were seeded in six-well plates and treated with compounds at a concentration of 5 μM for 48 h. The cells were then harvested by trypsinization and washed twice with cold PBS. After centrifugation and removal of the supernatants, cells were resuspended in 400 μL of 1× binding buffer, which was then added to 5 μL of annexin V-FITC and incubated at room temperature for 15 min. After adding 10 μL of PI, the cells were incubated at room temperature for another 15 min in the dark. The stained cells were analyzed by a flow cytometer (BD Accuri C6).

Molecular Modeling. Selected compounds were docked into the active site of Top1 by a similar procedure as described previously.[45] The X-ray crystallographic structure of the ATPase domain of human Top2α (PDB code: 1ZXM[78]) was applied using the CHARMm force field (Discovery Studio 3.0 software package[79]), and the residues were corrected for physiological pH. Mg ion and two water molecules (927 and 928) were conserved. The binding region was defined as all the atoms that are 12 Å around the centroid of ADPNP in the crystal structure. Docking runs were performed using the program GOLD 5.0.1 on a Linux PC, and the standard default settings were utilized with the following exceptions: (i) maximal ligand flexibility was allowed, (ii) a default maximum of 10000 genetic operations was performed, and (iii) water molecules were allowed to toggle "on" during the docking. Early termination was allowed if the top three solutions were within rmsd value of 1.5 Å. ChemPLP was used for the scoring of the final poses. MD calculations were used to validate the binding poses obtained from molecular docking. Desmond[80−83] (version Desmond_Maestro_academic-2009−02, http://www.deshawresearch.com) was used to carry out all the simulations, and the detailed protocols were similar to those in our previous studies.[45] The results indicated that the docked configuration and stable conformation after MD calculations were similar, with rmsd values lower than 2 Å, and important hydrogen bonding interactions were retained.

In Vivo Antitumor Activity. BALB/C nude male mice (certificate SCXK-2007−0005, weighing 18−20 g) were obtained from the Shanghai Experimental Animal Center, Chinese Academy of Sciences. A549 lung cancer cell suspensions or HCT116 colon cancer cell suspensions were implanted subcutaneously into the right axilla region of mice. Treatment was begun when implanted tumors had reached a volume of about 100−300 mm^3 (after 17 days). The animals were randomized into appropriate groups (six animals/treatment and eight animals for the control group) and administered by ip injection once on day 17 after implantation of cells. Tumor volumes were monitored by caliper measurement of the length and width and calculated using the formula of $TV = {}^1/_2 \times a \times b^2$, where a is the tumor length and b is the width. Tumor volumes and body weights were monitored every 4 days over the course of treatment. Mice were sacrificed on day 30−33 after implantation of cells, and tumors were removed and recorded for analysis.

■ ASSOCIATED CONTENT

Supporting Information

List of potential targets for compound **14d**, relative inhibition rate of the tested derivatives for Top1 and Top2α, experimental protocol and results of the Hoechst 33258 displacement experiment, structural characterization of target compounds, and the change of body weight for the nude mice treated with selected derivatives. This material is available free of charge via the Internet at http://pubs.acs.org.

■ AUTHOR INFORMATION

Corresponding Author

*For C.Q.S.: phone/fax, 86-21-81871239, E-mail, shengcq@hotmail.com. For W.N.Z.: phone/fax, 86-21-81871243; E-mail, zhangwnk@hotmail.com.

Author Contributions

†These two authors contributed equally to this work.

Notes

The authors declare no competing financial interest.

■ ACKNOWLEDGMENTS

This work was supported in part by the National Natural Science Foundation of China (grant 81222044, 30930107), the 863 Hi-Tech Program of China (grant 2012AA020302), Shanghai Rising-Star Program (grant 12QH1402600), Science and Technology Commission of Shanghai (grant 11431920402), and Shanghai Municipal Health Bureau (grant XYQ2011038). We gratefully acknowledge technical support from Dr. Xiaofeng Liu and Prof. Honglin Li (School of Pharmacy, East China University of Science and Technology, P. R. China) for in silico target identification.

■ ABBREVIATIONS USED

CPT, camptothecin; Top1, topoisomerase I; Top2, topoisomerase II; TPT, topotecan; IRT, irinotecan; SAR, structure−activity relationship; IBX, 2-iodoxybenzoic acid; MD, molecular dynamics

■ REFERENCES

(1) Newman, D. J.; Cragg, G. M.; Snader, K. M. Natural products as sources of new drugs over the period 1981−2002. *J. Nat. Prod.* **2003**, *66*, 1022−1037.

(2) Newman, D. J.; Cragg, G. M. Natural products as sources of new drugs over the last 25 years. *J. Nat. Prod.* **2007**, *70*, 461−477.

(3) Balamurugan, R.; Dekker, F. J.; Waldmann, H. Design of compound libraries based on natural product scaffolds and protein structure similarity clustering (PSSC). *Mol. Biosyst.* **2005**, *1*, 36−45.

(4) Oberlies, N. H.; Kroll, D. J. Camptothecin and taxol: historic achievements in natural products research. *J. Nat. Prod.* **2004**, *67*, 129−135.

(5) Wall, M. E.; Wani, M. C.; Cook, C. E.; Palmer, K. H.; McPhail, A. T.; Sim, G. A. The Isolation and Structure of Camptothecin, a Novel

Alkaloidal Leukemia and Tumor Inhibitor from Camptotheca Acuminata. *J. Am. Chem. Soc.* **1966**, *88*, 3888−3890.
(6) Hsiang, Y. H.; Hertzberg, R.; Hecht, S.; Liu, L. F. Camptothecin induces protein-linked DNA breaks via mammalian DNA topoisomerase I. *J. Biol. Chem.* **1985**, *260*, 14873−14878.
(7) Kingsbury, W. D.; Boehm, J. C.; Jakas, D. R.; Holden, K. G.; Hecht, S. M.; Gallagher, G.; Caranfa, M. J.; McCabe, F. L.; Faucette, L. F.; Johnson, R. K.; et al. Synthesis of water-soluble (aminoalkyl)-camptothecin analogues: inhibition of topoisomerase I and antitumor activity. *J. Med. Chem.* **1991**, *34*, 98−107.
(8) Garcia-Carbonero, R.; Supko, J. G. Current perspectives on the clinical experience, pharmacology, and continued development of the camptothecins. *Clin. Cancer Res.* **2002**, *8*, 641−661.
(9) Giovanella, B. C.; Stehlin, J. S.; Hinz, H. R.; Kozielski, A. J.; Harris, N. J.; Vardeman, D. M. Preclinical evaluation of the anticancer activity and toxicity of 9-nitro-20(*S*)-camptothecin (Rubitecan). *Int. J. Oncol.* **2002**, *20*, 81−88.
(10) Eckhardt, S. G.; Baker, S. D.; Eckardt, J. R.; Burke, T. G.; Warner, D. L.; Kuhn, J. G.; Rodriguez, G.; Fields, S.; Thurman, A.; Smith, L.; Rothenberg, M. L.; White, L.; Wissel, P.; Kunka, R.; DePee, S.; Littlefield, D.; Burris, H. A.; Von Hoff, D. D.; Rowinsky, E. K.; Phase, I and pharmacokinetic study of GI147211, a water-soluble camptothecin analogue, administered for five consecutive days every three weeks. *Clin. Cancer Res.* **1998**, *4*, 595−604.
(11) Minami, H.; Fujii, H.; Igarashi, T.; Itoh, K.; Tamanoi, K.; Oguma, T.; Sasaki, Y. Phase I and pharmacological study of a new camptothecin derivative, exatecan mesylate (DX-8951f), infused over 30 minutes every three weeks. *Clin. Cancer Res.* **2001**, *7*, 3056−3064.
(12) Liao, J. F.; Chen, C. F.; Chow, S. Y. Pharmacological studies of Chinese herbs. (9) Pharmacological effects of *Evodiae fructus*. *J. Formosan Med. Assoc.* **1981**, *80*, 30−38.
(13) Yu, X.; Wu, D. Z.; Yuan, J. Y.; Zhang, R. R.; Hu, Z. B. Gastroprotective effect of fructus evodiae water extract on ethanol-induced gastric lesions in rats. *Am. J. Chin. Med.* **2006**, *34*, 1027−1035.
(14) Chiou, W. F.; Sung, Y. J.; Liao, J. F.; Shum, A. Y.; Chen, C. F. Inhibitory effect of dehydroevodiamine and evodiamine on nitric oxide production in cultured murine macrophages. *J. Nat. Prod.* **1997**, *60*, 708−711.
(15) Ko, H. C.; Wang, Y. H.; Liou, K. T.; Chen, C. M.; Chen, C. H.; Wang, W. Y.; Chang, S.; Hou, Y. C.; Chen, K. T.; Chen, C. F.; Shen, Y. C. Anti-inflammatory effects and mechanisms of the ethanol extract of *Evodia rutaecarpa* and its bioactive components on neutrophils and microglial cells. *Eur. J. Pharmacol.* **2007**, *555*, 211−217.
(16) Liu, Y. N.; Pan, S. L.; Liao, C. H.; Huang, D. Y.; Guh, J. H.; Peng, C. Y.; Chang, Y. L.; Teng, C. M. Evodiamine represses hypoxia-induced inflammatory proteins expression and hypoxia-inducible factor 1alpha accumulation in RAW264.7. *Shock* **2009**, *32*, 263−269.
(17) Kobayashi, Y.; Nakano, Y.; Kizaki, M.; Hoshikuma, K.; Yokoo, Y.; Kamiya, T. Capsaicin-like anti-obese activities of evodiamine from fruits of *Evodia rutaecarpa*, a vanilloid receptor agonist. *Planta Med.* **2001**, *67*, 628−633.
(18) Bak, E. J.; Park, H. G.; Kim, J. M.; Yoo, Y. J.; Cha, J. H. Inhibitory effect of evodiamine alone and in combination with rosiglitazone on in vitro adipocyte differentiation and in vivo obesity related to diabetes. *Int. J. Obes.* **2010**, *34*, 250−260.
(19) Wang, T.; Wang, Y.; Kontani, Y.; Kobayashi, Y.; Sato, Y.; Mori, N.; Yamashita, H. Evodiamine improves diet-induced obesity in a uncoupling protein-1-independent manner: involvement of antiadipogenic mechanism and extracellularly regulated kinase/mitogen-activated protein kinase signaling. *Endocrinology* **2008**, *149*, 358−366.
(20) Wang, T.; Wang, Y.; Yamashita, H. Evodiamine inhibits adipogenesis via the EGFR-PKCalpha-ERK signaling pathway. *FEBS Lett.* **2009**, *583*, 3655−3659.
(21) Jiang, J.; Hu, C. Evodiamine: a novel anti-cancer alkaloid from *Evodia rutaecarpa*. *Molecules* **2009**, *14*, 1852−1859.
(22) Fei, X. F.; Wang, B. X.; Li, T. J.; Tashiro, S.; Minami, M.; Xing, D. J.; Ikejima, T. Evodiamine, a constituent of *Evodiae fructus*, induces anti-proliferating effects in tumor cells. *Cancer Sci.* **2003**, *94*, 92−98.
(23) Kan, S. F.; Huang, W. J.; Lin, L. C.; Wang, P. S. Inhibitory effects of evodiamine on the growth of human prostate cancer cell line LNCaP. *Int. J. Cancer* **2004**, *110*, 641−651.
(24) Liao, C. H.; Pan, S. L.; Guh, J. H.; Chang, Y. L.; Pai, H. C.; Lin, C. H.; Teng, C. M. Antitumor mechanism of evodiamine, a constituent from Chinese herb *Evodiae fructus*, in human multiple-drug resistant breast cancer NCI/ADR-RES cells in vitro and in vivo. *Carcinogenesis* **2005**, *26*, 968−975.
(25) Yang, Z. G.; Chen, A. Q.; Liu, B. Antiproliferation and apoptosis induced by evodiamine in human colorectal carcinoma cells (COLO-205). *Chem. Biodivers.* **2009**, *6*, 924−933.
(26) Kan, S. F.; Yu, C. H.; Pu, H. F.; Hsu, J. M.; Chen, M. J.; Wang, P. S. Anti-proliferative effects of evodiamine on human prostate cancer cell lines DU145 and PC3. *J. Cell. Biochem.* **2007**, *101*, 44−56.
(27) Chen, M. C.; Yu, C. H.; Wang, S. W.; Pu, H. F.; Kan, S. F.; Lin, L. C.; Chi, C. W.; Ho, L. L.; Lee, C. H.; Wang, P. S. Anti-proliferative effects of evodiamine on human thyroid cancer cell line ARO. *J. Cell. Biochem.* **2010**, *110*, 1495−1503.
(28) Zhang, C.; Fan, X.; Xu, X.; Yang, X.; Wang, X.; Liang, H. P. Evodiamine induces caspase-dependent apoptosis and S phase arrest in human colon lovo cells. *Anticancer Drugs* **2010**, *21*, 766−776.
(29) Lee, T. J.; Kim, E. J.; Kim, S.; Jung, E. M.; Park, J. W.; Jeong, S. H.; Park, S. E.; Yoo, Y. H.; Kwon, T. K. Caspase-dependent and caspase-independent apoptosis induced by evodiamine in human leukemic U937 cells. *Mol. Cancer Ther.* **2006**, *5*, 2398−2407.
(30) Huang, H.; Zhang, Y.; Liu, X.; Li, Z.; Xu, W.; He, S.; Huang, Y.; Zhang, H. Acid sphingomyelinase contributes to evodiamine-induced apoptosis in human gastric cancer SGC-7901 cells. *DNA Cell Biol.* **2011**, *30*, 407−412.
(31) Wang, C.; Li, S.; Wang, M. W. Evodiamine-induced human melanoma A375-S2 cell death was mediated by PI3K/Akt/caspase and Fas-L/NF-kappaB signaling pathways and augmented by ubiquitin−proteasome inhibition. *Toxicol. in Vitro* **2010**, *24*, 898−904.
(32) Ogasawara, M.; Matsubara, T.; Suzuki, H. Inhibitory effects of evodiamine on in vitro invasion and experimental lung metastasis of murine colon cancer cells. *Biol. Pharm. Bull.* **2001**, *24*, 917−920.
(33) Ogasawara, M.; Matsubara, T.; Suzuki, H. Screening of natural compounds for inhibitory activity on colon cancer cell migration. *Biol. Pharm. Bull.* **2001**, *24*, 720−723.
(34) Yang, X. W.; Zhang, H.; Li, M.; Du, L. J.; Yang, Z.; Xiao, S. Y. Studies on the alkaloid constituents of *Evodia rutaecarpa* (Juss) Benth var. bodinaieri (Dode) Huang and their acute toxicity in mice. *J. Asian Nat. Prod. Res.* **2006**, *8*, 697−703.
(35) Lipinski, C. A.; Lombardo, F.; Dominy, B. W.; Feeney, P. J. Experimental and computational approaches to estimate solubility and permeability in drug discovery and development settings. *Adv. Drug Deliv. Rev.* **2001**, *46*, 3−26.
(36) Hann, M. M.; Oprea, T. I. Pursuing the leadlikeness concept in pharmaceutical research. *Curr. Opin. Chem. Biol.* **2004**, *8*, 255−263.
(37) Oprea, T. I.; Davis, A. M.; Teague, S. J.; Leeson, P. D. Is there a difference between leads and drugs? A historical perspective. *J. Chem. Inf. Comput. Sci.* **2001**, *41*, 1308−1315.
(38) Manly, C. J.; Chandrasekhar, J.; Ochterski, J. W.; Hammer, J. D.; Warfield, B. B. Strategies and tactics for optimizing the Hit-to-Lead process and beyond—a computational chemistry perspective. *Drug Discovery Today* **2008**, *13*, 99−109.
(39) Baruah, B.; Dasu, K.; Vaitilingam, B.; Mamnoor, P.; Venkata, P. P.; Rajagopal, S.; Yeleswarapu, K. R. Synthesis and cytotoxic activity of novel quinazolino-beta-carboline-5-one derivatives. *Bioorg. Med. Chem.* **2004**, *12*, 1991−1994.
(40) Chen, Z.; Hu, G.; Li, D.; Chen, J.; Li, Y.; Zhou, H.; Xie, Y. Synthesis and vasodilator effects of rutaecarpine analogues which might be involved transient receptor potential vanilloid subfamily, member 1 (TRPV1). *Bioorg. Med. Chem.* **2009**, *17*, 2351−2359.
(41) Decker, M. Novel inhibitors of acetyl- and butyrylcholinesterase derived from the alkaloids dehydroevodiamine and rutaecarpine. *Eur. J. Med. Chem.* **2005**, *40*, 305−313.

(42) Hong, Y. H.; Lee, W. J.; Lee, S. H.; Son, J. K.; Kim, H. L.; Nam, J. M.; Kwon, Y.; Jahng, Y. Synthesis and biological properties of benzo-annulated rutaecarpines. *Biol. Pharm. Bull.* **2010**, *33*, 1704−1709.
(43) Wang, B.; Mai, Y. C.; Li, Y.; Hou, J. Q.; Huang, S. L.; Ou, T. M.; Tan, J. H.; An, L. K.; Li, D.; Gu, L. Q.; Huang, Z. S. Synthesis and evaluation of novel rutaecarpine derivatives and related alkaloids derivatives as selective acetylcholinesterase inhibitors. *Eur. J. Med. Chem.* **2010**, *45*, 1415−1423.
(44) Pin, F.; Comesse, S.; Daïch, A. Intramolecular *N*-aza-amidoalkylation in association with WitkopeWinterfeldt oxidation as the key step to synthesize Luotonin-A analogues. *Tetrahedron* **2011**, *67*, 5564−5571.
(45) Dong, G.; Sheng, C.; Wang, S.; Miao, Z.; Yao, J.; Zhang, W. Selection of evodiamine as a novel topoisomerase I inhibitor by structure-based virtual screening and hit optimization of evodiamine derivatives as antitumor agents. *J. Med. Chem.* **2010**, *53*, 7521−7531.
(46) Nakayama, A.; N., K.; M., k.; H., T. Straightforward asymmetric total synthesis of (+)-evodiamine, a major indole alkloid in herbal medicine "Wu Zhu Yu". *Heterocycles* **2008**, *76*, 861−865.
(47) Fujii, A.; Hashiguchi, S.; Uematsu, N.; Ikariya, T.; Noyori, R. Ruthenium(II)-Catalyzed Asymmetric Transfer Hydrogenation of Ketones Using a Formic Acid−Triethylamine Mixture. *J. Am. Chem. Soc.* **1996**, *118*, 2521−2522.
(48) Lee, S. H.; Son, J. K.; Jeong, B. S.; Jeong, T. C.; Chang, H. W.; Lee, E. S.; Jahng, Y. Progress in the studies on rutaecarpine. *Molecules* **2008**, *13*, 272−300.
(49) Jones, G.; Willett, P.; Glen, R. C.; Leach, A. R.; Taylor, R. Development and validation of a genetic algorithm for flexible docking. *J. Mol. Biol.* **1997**, *267*, 727−748.
(50) *Desmond_Maestro_academic-2009−02*; http://www.deshawresearch.com.
(51) Liu, X.; Jiang, H.; Li, H. SHAFTS: a hybrid approach for 3D molecular similarity calculation. 1. Method and assessment of virtual screening. *J. Chem. Inf. Model.* **2011**, *51*, 2372−2385.
(52) Lu, W.; Liu, X.; Cao, X.; Xue, M.; Liu, K.; Zhao, Z.; Shen, X.; Jiang, H.; Xu, Y.; Huang, J.; Li, H. SHAFTS: a hybrid approach for 3D molecular similarity calculation. 2. Prospective case study in the discovery of diverse p90 ribosomal S6 protein kinase 2 inhibitors to suppress cell migration. *J. Med. Chem.* **2011**, *54*, 3564−3574.
(53) *MDL Drug Data Report*; Symyx Technologies, Inc.: Sunnyvale, CA.
(54) Nitiss, J. L. Targeting DNA topoisomerase II in cancer chemotherapy. *Nature Rev. Cancer* **2009**, *9*, 338−350.
(55) Jun, K. Y.; Lee, E. Y.; Jung, M. J.; Lee, O. H.; Lee, E. S.; Park Choo, H. Y.; Na, Y.; Kwon, Y. Synthesis, biological evaluation, and molecular docking study of 3-(3′-heteroatom substituted-2′-hydroxy-1′-propyloxy) xanthone analogues as novel topoisomerase II alpha catalytic inhibitor. *Eur. J. Med. Chem.* **2011**, *46*, 1964−1971.
(56) Graves, D. E. Drug−DNA Interactions. *Methods Mol. Biol.* **2001**, *95*, 161−169.
(57) Peixoto, P.; Bailly, C.; Helene, M.; David-Cordonnier, M.-H. Topoisomerase I-mediated DNA relaxation as a tool to study intercalation of small molecules into supercoiled DNA. In *Drug−DNA Interaction Protocols*, 2nd ed.; Fox, K. R., Ed.; Humana Press; Totowa, NJ, 2010; Vol. *613*, pp 235−256.
(58) Suh, D.; Chaires, J. B. Criteria for the mode of binding of DNA binding agents. *Bioorg. Med. Chem.* **1995**, *3*, 723−728.
(59) Palchaudhuri, R.; Hergenrother, P. J. DNA as a target for anticancer compounds: methods to determine the mode of binding and the mechanism of action. *Curr. Opin. Biotechnol.* **2007**, *18*, 497−503.
(60) Perrin, D.; van Hille, B.; Barret, J. M.; Kruczynski, A.; Etievant, C.; Imbert, T.; Hill, B. T. F 11782, a novel epipodophylloid non-intercalating dual catalytic inhibitor of topoisomerases I and II with an original mechanism of action. *Biochem. Pharmacol.* **2000**, *59*, 807−819.
(61) Huang, H.; Chen, Q.; Ku, X.; Meng, L.; Lin, L.; Wang, X.; Zhu, C.; Wang, Y.; Chen, Z.; Li, M.; Jiang, H.; Chen, K.; Ding, J.; Liu, H. A series of alpha-heterocyclic carboxaldehyde thiosemicarbazones inhibit topoisomerase IIalpha catalytic activity. *J. Med. Chem.* **2010**, *53*, 3048−3064.
(62) Vos, S. M.; Tretter, E. M.; Schmidt, B. H.; Berger, J. M. All tangled up: how cells direct, manage and exploit topoisomerase function. *Nature Rev. Mol. Cell Biol.* **2011**, *12*, 827−841.
(63) Pommier, Y. DNA topoisomerase I inhibitors: chemistry, biology, and interfacial inhibition. *Chem. Rev.* **2009**, *109*, 2894−2902.
(64) Bailly, C. Contemporary Challenges in the Design of Topoisomerase II Inhibitors for Cancer Chemotherapy. *Chem. Rev.* **2012**, *112*, 3611−3640.
(65) Denny, W. A.; Baguley, B. C. Dual topoisomerase I/II inhibitors in cancer therapy. *Curr. Top. Med. Chem.* **2003**, *3*, 339−353.
(66) Dallavalle, S.; Gattinoni, S.; Mazzini, S.; Scaglioni, L.; Merlini, L.; Tinelli, S.; Beretta, G. L.; Zunino, F. Synthesis and cytotoxic activity of a new series of topoisomerase I inhibitors. *Bioorg. Med. Chem. Lett.* **2008**, *18*, 1484−1489.
(67) Salerno, S.; Da Settimo, F.; Taliani, S.; Simorini, F.; La Motta, C.; Fornaciari, G.; Marini, A. M. Recent advances in the development of dual topoisomerase I and II inhibitors as anticancer drugs. *Curr. Med. Chem.* **2010**, *17*, 4270−4290.
(68) Sheng, C.; Miao, Z.; Zhang, W. New strategies in the discovery of novel non-camptothecin topoisomerase I inhibitors. *Curr. Med. Chem.* **2011**, *18*, 4389−4409.
(69) Martin, S. F.; Benage, B.; Hunter, J. E. A concise strategy for the syntheses of indole alkaloids of the heteroyohimboid and corynantheioid families. Total syntheses of (±)-tetrahydroalstonine, (±)-cathenamine and (±)-geissoschizine. *J. Am. Chem. Soc.* **1988**, *110*, 5925−5927.
(70) D'Souza, A. M.; Spiccia, N.; Basutto, J.; Jokisz, P.; Wong, L. S.; Meyer, A. G.; Holmes, A. B.; White, J. M.; Ryan, J. H. 1,3-Dipolar cycloaddition−decarboxylation reactions of an azomethine ylide with isatoic anhydrides: formation of novel benzodiazepinones. *Org. Lett.* **2011**, *13*, 486−489.
(71) Aleksic, M.; Bertosa, B.; Nhili, R.; Uzelac, L.; Jarak, I.; Depauw, S.; David-Cordonnier, M. H.; Kralj, M.; Tomic, S.; Karminski-Zamola, G. Novel Substituted Benzothiophene and Thienothiophene Carboxanilides and Quinolones: Synthesis, Photochemical Synthesis, DNA-Binding Properties, Antitumor Evaluation and 3D-Derived QSAR Analysis. *J. Med. Chem.* **2012**, *55*, 5044−5060.
(72) Wang, P.; Leung, C. H.; Ma, D. L.; Lu, W.; Che, C. M. Organoplatinum(II) complexes with nucleobase motifs as inhibitors of human topoisomerase II catalytic activity. *Chem. Asian J.* **2010**, *5*, 2271−2280.
(73) Li, X.; Lin, Y.; Wang, Q.; Yuan, Y.; Zhang, H.; Qian, X. The novel anti-tumor agents of 4-triazol-1,8-naphthalimides: synthesis, cytotoxicity, DNA intercalation and photocleavage. *Eur. J. Med. Chem.* **2011**, *46*, 1274−1279.
(74) Baviskar, A. T.; Madaan, C.; Preet, R.; Mohapatra, P.; Jain, V.; Agarwal, A.; Guchhait, S. K.; Kundu, C. N.; Banerjee, U. C.; Bharatam, P. V. N-Fused imidazoles as novel anticancer agents that inhibit catalytic activity of topoisomerase IIalpha and induce apoptosis in G1/S phase. *J. Med. Chem.* **2011**, *54*, 5013−5030.
(75) Du, L.; Liu, H. C.; Fu, W.; Li, D. H.; Pan, Q. M.; Zhu, T. J.; Geng, M. Y.; Gu, Q. Q. Unprecedented citrinin trimer tricitinol B functions as a novel topoisomerase IIalpha inhibitor. *J. Med. Chem.* **2011**, *54*, 5796−5810.
(76) Marshall, K. M.; Holden, J. A.; Koller, A.; Kashman, Y.; Copp, B. R.; Barrows, L. R. AK37: the first pyridoacridine described capable of stabilizing the topoisomerase I cleavable complex. *Anticancer Drugs* **2004**, *15*, 907−913.
(77) Routier, S.; Peixoto, P.; Merour, J. Y.; Coudert, G.; Dias, N.; Bailly, C.; Pierre, A.; Leonce, S.; Caignard, D. H. Synthesis and biological evaluation of novel naphthocarbazoles as potential anticancer agents. *J. Med. Chem.* **2005**, *48*, 1401−1413.
(78) Wei, H.; Ruthenburg, A. J.; Bechis, S. K.; Verdine, G. L. Nucleotide-dependent domain movement in the ATPase domain of a human type IIA DNA topoisomerase. *J. Biol. Chem.* **2005**, *280*, 37041−37047.
(79) *Discovery Studio 3.0*; Accelrys Software Inc.: San Diego, CA, 2010; http://www.accelrys.com.

(80) Shaw, D. E. A fast, scalable method for the parallel evaluation of distance-limited pairwise particle interactions. *J. Comput. Chem.* **2005**, *26*, 1318−1328.
(81) Bowers, K. J.; Chow, E.; Xu, H.; Dror, R. O.; Eastwood, M. P.; Gregersen, B. A.; Klepeis, J. L.; Kolossváry, I.; Moraes, M. A.; Sacerdoti, J. K.; Shan, Y.; Shaw, D. E. Scalable Algorithms for Molecular Dynamics Simulations on Commodity Clusters. Proceedings of the ACM/IEEE Conference on Supercomputing (SC06), Tampa, Florida, November 11−17, 2006.
(82) Bowers, K. J.; Dror, R. O.; Shaw, D. E. The midpoint method for parallelization of particle simulations. *J. Chem. Phys.* **2006**, *124*, 184109.
(83) Bowers, K. J.; Dror, R. O.; Shaw, D. E. Zonal Methods for the Parallel Execution of Range-Limited N-Body Simulations. *J. Comput. Phys.* **2007**, *221*, 303−329.